

**ENHANCED BINDING AND CONFORMATIONAL SELECTIVITY  
IN AFFINITY CAPILLARY ELECTROPHORESIS USING A  
WATER-SOLUBLE RESORCIN[4]ARENE AS INTRINSIC BUFFER  
AND ELECTROKINETIC HOST**

**ENHANCED BINDING AND CONFORMATIONAL SELECTIVITY  
IN AFFINITY CAPILLARY ELECTROPHORESIS USING A  
WATER-SOLUBLE RESORCIN[4]ARENE AS INTRINSIC BUFFER  
AND ELECTROKINETIC HOST**

By

**SHEEBA SAMSON**

A Thesis

Submitted to the school of Graduate Studies

In Partial Fulfillment of the Requirements

for the Degree

Master of Science

McMaster University

© Copyright by Sheeba Samson, September 2005

**MASTER OF SCIENCE  
McMaster University  
(Chemistry)  
Hamilton, Ontario**

**TITLE: Enhanced binding and conformational selectivity in affinity capillary electrophoresis using a water-soluble resorcin[4]arene as intrinsic buffer and electrokinetic host**

**AUTHOR: Sheeba Samson**

**SUPERVISOR: Dr. Philip Britz-McKibbin**

**NUMBER OF PAGES: 100**

***For my parents and husband***

## ABSTRACT

Affinity capillary electrophoresis (ACE) is a versatile technique for assessing non-covalent molecular interactions in free solution provided that there are significant changes in apparent analyte mobility as a result of specific complexation. The thermodynamics of receptor binding are vital for controlling the selectivity in molecular recognition, which are dependent on the electrolyte composition of solution. In addition, the conformational properties of the complex (*e.g.*, size, shape) can also contribute a secondary influence on receptor selectivity that has been relatively unexplored in ACE to date. In this study, dynamic 1:1 host-guest inclusion complexation involving an anionic resorcin[4]arene with a group of neutral corticosteroids was examined by ACE, where the macrocycle serves as both an intrinsic buffer and electrokinetic host. The tetraethylsulphonate derivative of 2-methylresorcin[4]arene (TESMR) was first synthesized via an acid-catalyzed condensation reaction, which was then fully characterized in terms of its weak acidity ( $pK_a$ ), mobility, UV spectral and buffer capacity properties. TESMR solutions were demonstrated to have stable intrinsic buffer and ion transport properties at pH 7.5 even at low ionic strength. It was determined that over a 200 % enhancement in the apparent binding constant ( $K_B$ ) was realized by ACE when using TESMR as an intrinsic buffer at pH 7.5 relative to an extrinsic sodium phosphate buffer system, which was also confirmed by  $^1H$ -NMR. The coupling of thermodynamic ( $K_B$ ) and electrokinetic ( $\mu_{ep, AC}$ ) factors associated with complex formation in buffered aqueous solutions that minimize the effects of extrinsic electrolytes serves to enhance enthalpy-driven molecular recognition processes by ACE.

## **ACKNOWLEDGEMENTS**

Countless thanks to God for blessing me with the strength, courage and wisdom to complete my thesis. I feel great pleasure in expressing my profound gratitude to Dr. Philip Britz-McKibbin for his able guidance and skilled advice, which were a real source of inspiration for me during my research project. Dr. Britz, thank you very much for giving me the opportunity to work with you, for having confidence in me and for guiding me. I would also like to thank Dr. Capretta, Dr. Bain and Dr Hughes for all their help over the past couple of years. Many thanks to my lab mates and friends, Adam, Giselle, Elyse and Mohit for being there for me and for being great friends.

I would like to thank the most important people in my life, my parents, husband and siblings. I am really grateful for your encouragement, support and unconditional love, that guided me all these years. Guys, you are great and I love you a lot.

## TABLE OF CONTENTS

<b>Abstract</b> .....	<b>III</b>
<b>Acknowledgements</b> .....	<b>IV</b>
<b>Table of Contents</b> .....	<b>V</b>
<b>List of Figures</b> .....	<b>VIII</b>
<b>List of Tables</b> .....	<b>XI</b>
<b>List of Abbreviations</b> .....	<b>XII</b>
<b>CHAPTER 1</b> .....	<b>1</b>
<b>BACKGROUND</b> .....	<b>1</b>
1.1 Capillary electrophoresis (CE).....	<b>1</b>
<i>1.1.1 Historical background</i> .....	<b>2</b>
<i>1.1.2 Electrokinetic phenomena in CE</i> .....	<b>4</b>
<i>1.1.3 Electrophoretic mobility</i> .....	<b>4</b>
<i>1.1.4 Electroosmotic flow (EOF)</i> .....	<b>6</b>
<i>1.1.5 Apparent mobility</i> .....	<b>8</b>
1.2 Dynamic complexation using additives in CE.....	<b>10</b>
<i>1.2.1 SDS micelles</i> .....	<b>11</b>
<i>1.2.2 Cyclodextrins</i> .....	<b>13</b>
1.3 Calixarenes and resorcinarene macrocycles .....	<b>15</b>
<i>1.3.1 Historical perspective</i> .....	<b>15</b>
<i>1.3.2 Resorcin[4]arenes: Resorcinol-derived calixarenes</i> .....	<b>16</b>
<i>1.3.3 Stereochemical properties of resorcin[4]arenes</i> .....	<b>18</b>
1.4 Non-covalent interactions .....	<b>20</b>
<i>1.4.1 Ionic interactions</i> .....	<b>21</b>
<i>1.4.2 Hydrogen bonding</i> .....	<b>22</b>

<b>1.4.3 Dipole-dipole interactions: Dispersion forces</b> .....	23
<b>1.4.4 CH-<math>\pi</math> interactions</b> .....	24
<b>1.4.5 Hydrophobic interactions</b> .....	25
<b>1.4.6 <math>\pi - \pi</math> interactions</b> .....	26
1.5 Research objectives.....	27
1.6 References .....	29
<b>CHAPTER 2</b> .....	<b>33</b>
<b>SYNTHESIS AND CHARACTERIZATION OF A WATER-SOLUBLE RESORCIN[4]ARENE</b> .	<b>33</b>
2.1 Introduction.....	34
2.2 Experimental .....	36
<b>2.2.1 Chemicals</b> .....	36
<b>2.2.2 Apparatus and Procedure</b> .....	37
2.2.2.1 Synthesis of TESMR.....	37
2.2.2.2 Purification and desalting .....	38
2.2.2.3 Capillary electrophoresis.....	39
2.2.2.4 Characterization of TESMR .....	39
2.2.2.5 Spectroscopic measurements .....	40
2.3 Results and Discussion .....	40
<b>2.3.1 TESMR synthesis, purification and desalting</b> .....	40
<b>2.3.2 TESMR characterization</b> .....	43
<b>2.3.3 TESMR as an intrinsic buffer: <math>pK_a</math> Determination by CE</b> .....	46
<b>2.3.4 TESMR spectroscopic properties</b> .....	50
<b>2.3.5 TESMR buffer capacity</b> .....	53
2.4 Conclusion .....	55
2.5 References.....	56
<b>CHAPTER 3</b> .....	<b>58</b>
<b>ENHANCED BINDING AND CONFORMATIONAL SELECTIVITY IN AFFINITY CAPILLARY ELECTROPHORESIS USING A WATER-SOLUBLE RESORCIN[4]ARENE</b> .....	<b>58</b>

3.1 Introduction.....	59
3.2 Corticosteroids .....	62
3.3. Theory .....	63
3.4 Experimental .....	65
<b>3.4.1 Chemicals and Reagents</b> .....	65
<b>3.4.2 TESMR synthesis and purification</b> .....	66
<b>3.4.3 Capillary electrophoresis</b> .....	66
<b>3.4.4 <sup>1</sup>H-NMR</b> .....	68
<b>3.4.5 Computer molecular modeling</b> .....	69
3.5 Results and Discussion .....	70
<b>3.5.1 TESMR and steroid spectroscopic properties</b> .....	70
<b>3.5.2 TESMR as intrinsic buffer and electrokinetic host in ACE</b> .....	70
<b>3.5.3 Reduced apparent binding affinity in extrinsic buffer system</b> .....	74
<b>3.5.4 Conformational size selectivity in ACE</b> .....	77
3.6 Conclusion .....	81
3.7 References.....	82
<b>CHAPTER 4</b> .....	<b>85</b>
<b>FUTURE OUTLOOK</b> .....	<b>85</b>
4.1 Research plans .....	85
4.2 Influence of electrolyte composition .....	85
4.3 Anionic host:cationic guest model system.....	86
4.4 TESMR as a probe for indirect fluorescence detection .....	87

## LIST OF FIGURES

<b>Fig. 1.1</b> Schematic of the instrumental components of CE with UV detection .....	2
<b>Fig. 1.2</b> Debye-Hueckel-Stern model of the electric double layer highlighting (a) the diffuse double layer and (b) zeta potential that generates the EOF near the capillary surface under an external applied voltage. ....	7
<b>Fig. 1.3</b> (a) a flat electrokinetic EOF profile in CE and (b) a parabolic flow profile of a pressure-driven pump in HPLC .....	8
<b>Fig. 1.4</b> Schematic showing separation of a mixture of analytes based on their effective charge by CE: (a) sample injection, (b) zonal separation, (c) on-line detection and (d) electropherogram .....	9
<b>Fig. 1.5</b> Schematic of dynamic partitioning of neutral analytes using SDS as an additive in MEKC .....	12
<b>Fig. 1.6</b> (a) Chemical structure of $\beta$ -CD and (b) schematic of the truncated cone structure of the oligosaccharide macrocycle.....	14
<b>Fig. 1.7</b> Chemical structure of (a) phenol-derived and (b) resorcinol-derived calix [4] arenes. ....	16
<b>Fig. 1.8</b> Four diastereomeric configurations of resorcin[4]arenes: (a) rccc, (b) rctc, (c) rtct and (d) rett .....	19
<b>Fig. 1.9</b> Two major conformations of resorcin[4]arenes: (a) crown and (b) boat.....	19
<b>Fig. 1.10</b> Three different types of hydrogen bonding interactions involving a donor (D) and acceptor (A).....	24
<b>Fig. 1.11</b> Schematic of transient dipole-induced dispersion interactions (Van der Waal) in two neutral molecules resulting in a net attractive force.....	24
<b>Fig. 1.12</b> Schematic of several different types of CH- $\pi$ interactions.....	25
<b>Fig. 1.13</b> Schematic of three major types of CH- $\pi$ and $\pi$ - $\pi$ interactions involving aromatic systems (a) T-shaped, (b) face to face and (c) offset conformation.....	27
<b>Fig. 2.1</b> Three major types of water-soluble resorcin[4]arene derivatives including (a) Type 1, (b) Type 2 and (c) Type 3 based on the location of charged moiety.....	36

<b>Fig. 2.2</b> Pictorial illustration of TFF system that uses a porous 1000 Da MWCO filter for desalting.....	38
<b>Fig 2.3</b> (a) Measured conductivity as a function of TFF time using model 100mM NaCl solution and (b) measured conductivity as a function of TFF time using recrystallized TESMR product.....	42
<b>Fig.2.4</b> <sup>1</sup> H-NMR spectra of (a) crude and (b) desalted TESMR that highlight five different proton resonances indicative of the <i>all-cis</i> configuration of the macrocycle.....	44
<b>Fig. 2.5</b> Energy-minimized 3D conformation of TESMR highlighting its major structural features.....	44
<b>Fig. 2.6</b> CE purity assay of (a) crude and (b) TFF-desalted TESMR.....	45
<b>Fig. 2.7</b> (a) Triply and (b) quadruply charged molecular anions of TESMR by ESI-MS.....	45
<b>Fig. 2.8</b> Electropherograms demonstrating specific changes in analyte mobility as a function of buffer pH for determination of pK <sub>a</sub> by CE.....	47
<b>Fig. 2.9</b> Non-linear regression of mobility titration curves as determined by CE for the monoprotic acid (a) <i>m</i> -nitrophenol and the triprotic acid (b) TESMR.....	49
<b>Fig. 2.10</b> (a) Overlay of UV absorbance spectra of 20 μM TESMR as a function of buffer pH and (b) triplicate measurements of absorbance changes as a function of pH for pK <sub>a</sub> measurement.....	50
<b>Fig. 2.11</b> Fluorescence emission spectra of 2μM (a) TESMR and (b) Trp in dH <sub>2</sub> O using 266 nm excitation.....	52
<b>Fig. 2.12</b> Buffer capacity assessment by CE of 20 mM TESMR, pH 7.5 relative to phosphate buffer (buffer control) and dichromate (non-buffer control).....	54
<b>Fig. 3.1</b> Cyclopentaphenanthrene ring skeleton and numbering of steroid ring structure.....	62
<b>Fig. 3.2</b> Enzymatic conversion of hydrocortisone to cortisone.....	63
<b>Fig. 3.3</b> Overlay UV absorbance spectra of TESMR (solid line) and HC (dotted line).....	70
<b>Fig. 3.4</b> Chemical structures of the model corticosteroid guests (a) HC, (b) C and (c) CC.....	71
<b>Fig. 3.5</b> (a) Differential interaction of corticosteroids using TESMR as intrinsic buffer and electrokinetic host at pH 7.5 by ACE: (i) 0, (ii) 1, (iii) 2 and (iv) 4 mM TESMR. (b)	

Non-linear regression of the binding isotherms using average viscosity-corrected mobilities ( $n = 3$ ) of corticosteroids based on 1:1 dynamic complexation with TESMR as described in eq. 1. Guest numbering corresponds to: 1-HC, 2-C and 3-CC.....72

**Fig. 3.6**  $^1\text{H-NMR}$  complexation-induced chemical shifts of hydrocortisone in the presence of increasing concentrations of TESMR.....74

**Fig. 3.7** (a) Differential interaction of corticosteroids using TESMR as an electrokinetic host in 20 mM sodium phosphate buffer, pH 7.5 by ACE: (i) 0, (ii) 1, (iii) 2 and (iv) 4 mM TESMR. (b) Non-linear regression of the binding isotherms using average viscosity-corrected mobilities ( $n = 3$ ) of corticosteroids based on 1:1 dynamic inclusion complexation with TESMR as described in eq. 1.....75

**Fig. 3.8** Van't Hoff plot for the determination of enthalpy and entropy parameters involved in TESMR-HC interaction using the HC methyl-18 chemical shifts by  $^1\text{H NMR}$ .....76

**Fig. 3.9** Energy minimized stable conformation of TESMR (blue):HC (red) inclusion complex with H4, H18 and H19 residues in yellow (left→right).....80

**Fig. 4.1** Chemical structures of test guest analytes (a)tryptophan, (b)hydroxytryptophan, (c) tryptamine, (d) hydroxytryptamine .....86

**Fig. 4.2** Pictorial illustration of ACE with indirect LIF detection of DHEA by dynamic complexation with TESMR and displacement of the solvophobic dye dansylamide.....88

## **LIST OF TABLES**

<b>Table 1.1</b> Bond strengths involved in covalent and various non-covalent interactions...	22
<b>Table 2.1</b> Different purification stages of TESMR as determined by <sup>1</sup> H-NMR.....	45
<b>Table 2.2</b> Influence of solution properties on intrinsic fluorescence of TESMR.....	53
<b>Table 3.1</b> Enhanced molecular recognition of corticosteroids based on thermodynamic & conformational selectivity with TESMR as intrinsic buffer and electrokinetic host.....	78
<b>Table 3.2</b> <sup>1</sup> H-NMR binding isotherm data for HC using TESMR as an intrinsic buffer at pH 7.5.....	78

## LIST OF ABBREVIATIONS

ACE	Affinity capillary electrophoresis
C	Cortisone
CC	Corticosterone
CD	Cyclodextrin
CE	Capillary electrophoresis
EOF	Electroosmotic flow
TFF	Tangential flow filtration
ESI-MS	Electrospray ionization mass spectrometry
IEF	Isoelectric focusing
GE	Gel electrophoresis
HC	Hydrocortisone
HPLC	High performance liquid chromatography
$K_B$	Apparent binding constant
LIF	Laser-induced fluorescence detection
LINF	Laser-induced native fluorescence
$\Phi_F$	Fluorescence quantum efficiency
$\nu$	Relative viscosity-correction factor
MEKC	Micellar electrokinetic chromatography
$\mu_{ep, A}$	Analyte electrophoretic mobility
$\mu_{eo}$	Electroosmotic mobility
$\mu^A$	Apparent analyte mobility
$(1 - \mu_{ep, AC} / \mu_{ep, C})$	Relative change in complexation-induced mobility
PAGE	Polyacrylamide gel electrophoresis
$Q_{eff}$	Effective ion charge
$R_H$	Hydrodynamic radius
SDS	Sodium dodecyl sulphate
TESMR	Tetraethylsulphonate derivative of 2-methylresorcin[4]arene
Trp	Tryptophan

# CHAPTER 1

## Background

### 1.1 Capillary electrophoresis (CE)

Electrophoresis is generally defined as “the differential migration of ions in an electric field.” Capillary electrophoresis (CE) then, can be defined as a technique of performing electrophoretic separations in a narrow-bore, buffer-filled capillary with an internal diameter ranging from 25 to 100  $\mu\text{m}$  across which a high voltage is applied. The instrumentation required for CE is remarkably simple in design. A schematic of the instrumental components of CE is shown in Fig. 1.1. The major components include a high voltage power supply (0-30 kV), a polyimide-coated fused-silica capillary, two buffer reservoirs (inlet/outlet) that can accommodate both capillary ends and platinum electrodes, as well as an on-capillary photometric detector with direct computer control and data acquisition. The sample is injected onto the capillary by replacing one of the buffer reservoirs (inlet) with a sample reservoir, followed by an application of a positive pressure or an electric potential for a fixed period of time. The former injection type is referred to as hydrodynamic, whereas the later is electrokinetic injection. After sample injection, an electric potential is applied across the capillary and separation is performed. The analytes are then detected near the outlet of the capillary either using on-line UV absorbance or laser-induced fluorescence detection. In CE, the use of narrow capillaries as a format for performing separations has several important advantages, which include small sample volume requirements ( $< 10 \text{ nL}$ ) and minimal buffer consumption ( $< 0.5 \text{ mL}$ ) typically using aqueous solutions. Moreover, the high surface-to-volume ratio of

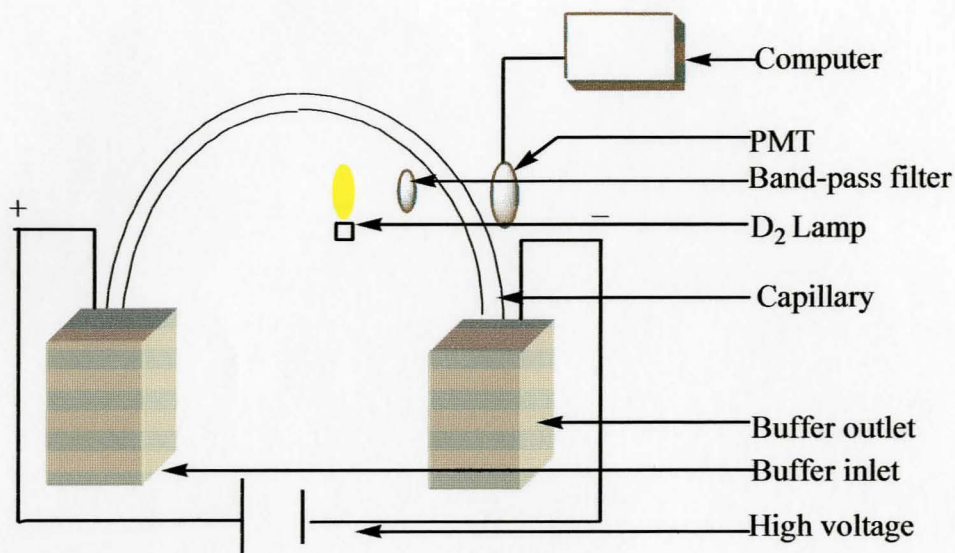


**Fig. 1.1** Schematic of the instrumental components of CE with UV detection

capillaries allows for very efficient dissipation of Joule heating generated by ion conduction, which permits the use of high voltages for rapid separations. CE is also amenable to high-throughput analyses with the advent of capillary array instruments that consist of 96 capillaries in a single instrumental platform, which was recently accredited to the early completion of DNA sequencing involved in the Human Genome Project [1]. Although CE is often considered in the context of a high resolution separation technique, there is increasing interest in applying it as a unique biophysical tool to investigate fundamental physicochemical parameters involving biomolecular interactions. This feature will represent a major focus in the present thesis.

### **1.1.1 Historical background**

Until the advent of CE, electrophoresis was historically performed primarily in a gel format by biochemists, which was conducive for high resolution separations of

biopolymers, such as protein and DNA. The term electrophoresis was first coined by Michaelis [2] in 1909, who introduced the principle of protein separations based on their isoelectric points in free solution. Vesterberg [3] later reported the use of ampholyte mixtures that had the ability to create stable pH gradients in a sieving gel matrix. In the early 1970s, 2D gel electrophoresis (GE) was then introduced by Dale and Latner [4] and Macko and Stegemann [5] which achieved high resolution orthogonal protein separations based on IEF and SDS-PAGE [6]. Although, 2D GE is still widely used today, its main disadvantages include labour intensive gel preparations, long separation times and low voltage applications due to excessive Joule heating, lack of automation with poor quantitative analysis. In addition, GE is not suitable for the high resolution separation of low molecular weight molecules. Meanwhile, there were increasing advances in the field of chromatography for small molecule separations, which indirectly aided in the development of CE, such as the introduction of narrow fused-silica capillaries for GC, as well as the use of on-line detectors and automated instrumentation in HPLC. In 1981, CE was first introduced by Jorgenson and Lukas [7] as a novel micro-separation platform for high resolution and rapid analyses of charged analytes. Terabe *et al.* [8, 9] later extended the usefulness of CE for neutral analytes by the use of charged micelles (*i.e.*, pseudo-stationary phases) as additives in the run buffer. Interest in CE has increased exponentially since the 1990s with the introduction of commercial instrumentation primarily due to its versatility for separating a wide variety of analytes ranging from small metal ions to high molecular weight proteins. This feature of CE is reflected by the several distinct modes of separation, such as affinity CE (ACE), micellar electrokinetic

chromatography (MEKC), cyclodextrin-mediated CE (CD-MCE), capillary electrochromatography (CEC) and isoelectric focusing capillary gel electrophoresis (IEF-CGE). In many cases, separation in CE is complementary to both HPLC and GC, which is well suited for rapid, high-throughput and high resolution separations of charged analytes. In addition, CE has the distinct advantage as a unique technique to characterize biomolecular interactions relative to chromatography, since there is no need for analyte/ligand immobilization or encapsulation chemistry as separation occurs via electromigration in free solution.

### **1.1.2 Electrokinetic phenomena in CE**

In CE, the migration of analytes is due to the superimposition of two major electrokinetic phenomena, namely the analyte electrophoretic mobility ( $\mu_{ep, A}$ ) and the electroosmotic mobility ( $\mu_{eo}$ ) or flow (EOF). The former term is a fundamental physicochemical property of an analyte, which determines overall selectivity, whereas the latter terms is a bulk property of the capillary and buffer system that acts as a natural electrokinetic pumping mechanism on all analytes.

### **1.1.3 Electrophoretic mobility**

The electrophoretic mobility is generally defined as the velocity of an ion ( $v$ ) per unit electric field strength ( $E$ ). In the case of a spherical ion,  $\mu_{ep, A}$  is based on the net balance of the electromotive and viscous drag force in solution, which can be described by the following equation [10]:

$$\mu_{ep,A} = \frac{v}{E} = \frac{Q_{eff}}{6\pi\eta R_H} \quad (1)$$

where,  $Q_{eff}$  is the effective charge of the analyte,  $\eta$  is the viscosity of the buffer, and  $R_H$  is the hydrodynamic radius of the analyte. Eq. 1 highlights the fact that selectivity in CE is based on differences in the direction and magnitude of  $\mu_{ep,A}$ , which is reflected by the effective charge to size ratio of an analyte in a buffer solution. For instance, small highly charged anions will have a high negative  $\mu_{ep,A}$ , whereas large minimally charged cations have low positive  $\mu_{ep,A}$ . In the case of neutral analytes with no intrinsic mobility, they will co-migrate with the EOF. Analytes that have similar chemical properties (*e.g.*, enantiomers) typically have the same  $\mu_{ep,A}$  in an achiral buffer environment. One of the major advantages of CE is that the intrinsic analyte mobility can be readily modified by changes in the composition of the run buffer, such as buffer type, pH, ionic strength, as well as the use of specific additives, such as cyclodextrins. Buffer pH is one of the most important parameters for improving resolution in CE that is especially relevant for weakly ionic analytes, such as amino acids. The buffer serves multiple functions in CE, such as controlling the degree of analyte ionization (*i.e.*,  $Q_{eff}$ ), resisting changes in buffer pH during separation due to water electrolysis, as well as acting as charged carriers to complete the electric circuit. It is important to note that  $\mu_{ep,A}$  represents an intrinsic physiochemical property of an analyte under defined conditions, such as temperature, solution viscosity and buffer pH. Changes in the measured analyte mobility by CE can be used in the determination of fundamental chemical parameters of analytes, such as  $pK_a$  [11, 12], diffusion constant [13] and apparent binding constant [14].

#### 1.1.4 Electroosmotic flow (EOF)

The EOF is a natural electrokinetic phenomenon that plays an important role in most CE separations. It is defined as the bulk flow of a solution in a buffer-filled capillary when a voltage is applied. Since the wall of fused-silica capillary in the presence of water consists of weakly acidic silanol moieties ( $pK_a \approx 3$ ), the capillary surface generally has a net negative charge above pH 4. However, under strongly acidic conditions (pH < 2), the silanol surface of the capillary is primarily protonated (neutral), resulting in a suppression of the EOF. Thus, the pH of the buffer is the major factor that controls the fraction of silanol ionization, which impacts the magnitude of the EOF reflected by the zeta potential ( $\zeta$ ). According to the Debye-Hueckel-Stern theory [10], an electric double layer of electrolytes is formed within a short distance (about 10-50 nm) of the negatively charged capillary wall, consisting of a rigid adsorbed layer of cations (Stern layer), followed by a diffuse layer of mobile cations and anions, as depicted in Fig. 1.2. Note that an excess of cations is distributed throughout the electric double layer in order to neutralize the excess negative charge of the capillary surface.  $\zeta$  is defined as the potential at the slipping plane between the rigid and diffuse double layer, which decreases exponentially away from the surface of the capillary. Upon application of an external voltage perpendicular to  $\zeta$ , there is a net migration of cations in the diffuse double layer towards the cathode. A stable EOF is generated in narrow capillary dimension capillaries (i.d. < 200  $\mu\text{m}$ ) since hydrated cations in the double layer transport bulk water via the cohesive nature of hydrogen bonding. Thus, the EOF acts as an intrinsic electrokinetic pumping mechanism to propel all analytes (cationic, anionic and neutral) towards the

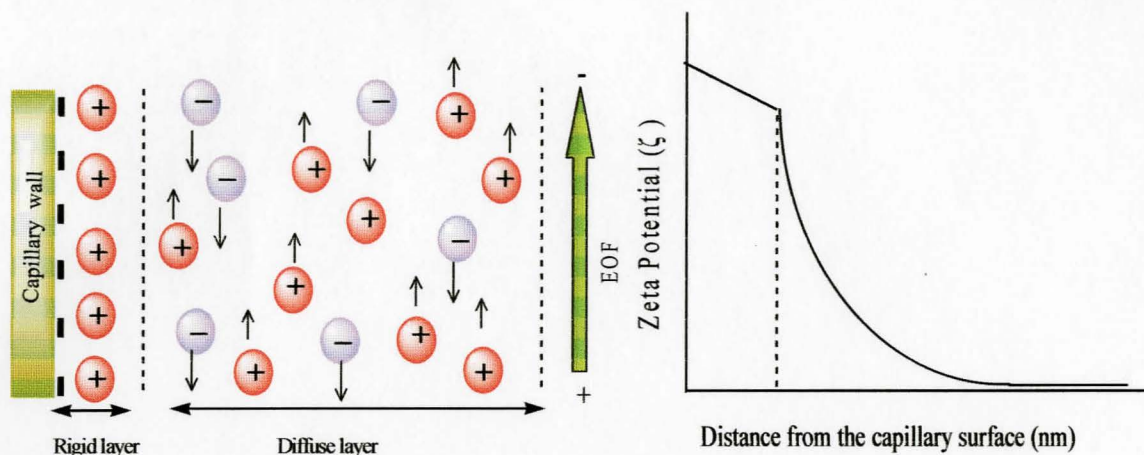


**Fig. 1.2** Debye-Hueckel-Stern model of the electric double layer highlighting (a) the diffuse double layer and (b) zeta potential that generates the EOF near the capillary surface under an external applied voltage.

detector. The EOF is defined along planar surfaces by the following equation [10]:

$$\mu_{eo} = \frac{\varepsilon\zeta}{4\pi\eta} \quad (2)$$

where,  $\varepsilon$  is the dielectric constant,  $\zeta$  is the zeta potential and  $\eta$  is the viscosity of the solution.  $\zeta$  is proportional to the charge density near the surface of the capillary wall, which depends on the pH and ionic strength of the buffer solution. In general, alkaline buffer solutions of low ionic strength generate a high  $\zeta$  and strong EOF. Under most condition in CE ( $\text{pH} > 4$ ), the magnitude of the EOF is greater than  $\mu_{ep, A}$ . An important feature of the EOF is that it has a near flat profile as shown in **Fig. 1.3 (a)**. The flat profile is attributed to the fact that the charge on the capillary is uniformly distributed so there is no pressure drop, hence generating a uniform flow velocity across the capillary (except in the Stern layer of adsorbed ions close to the capillary surface). In contrast, differential frictional forces in HPLC using an external pump cause a pressure drop across the capillary resulting in a parabolic flow profile, as shown in **Fig. 1.3 (b)**. The

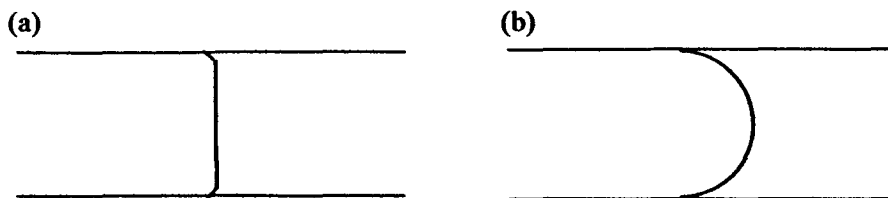


**Fig. 1.3** (a) A flat electrokinetic EOF profile in CE and (b) a parabolic flow profile of a pressure-driven pump in HPLC

flat profile of the EOF in CE is important because it minimizes longitudinal band dispersion, leading to higher separation efficiency (*e.g.*, plate numbers  $> 10^5$ ) and sharper analyte peaks with improved resolution, often over 10-fold greater than HPLC.

### 1.1.5 Apparent mobility

The apparent electrophoretic mobility of an analyte ( $\mu^A$ ) is the vector sum of  $\mu_{ep, A}$  and  $\mu_{eo}$  as described by the following equation:

$$\mu^A = \mu_{ep, A} + \mu_{eo} \quad (3)$$

A schematic of a typical CE separation involving three different analytes in a mixture, namely a cationic, an anionic and a neutral species is depicted in **Fig. 1.4**. The capillary is first rinsed and filled with run buffer using an external high pressure, followed by a short hydrodynamic injection of the sample mixture at the anodic end of the capillary, as shown in **Fig. 1.4 (a)**. Upon application of the voltage, the sample plug is transported by the EOF while discrete analyte zones are separated based on their different intrinsic  $\mu_{ep, A}$ . Note that the relative migration time is based on the effective charge state of the analyte, in the order of cation, neutral (co-migrates with EOF) and anion, as highlighted in **Fig.**

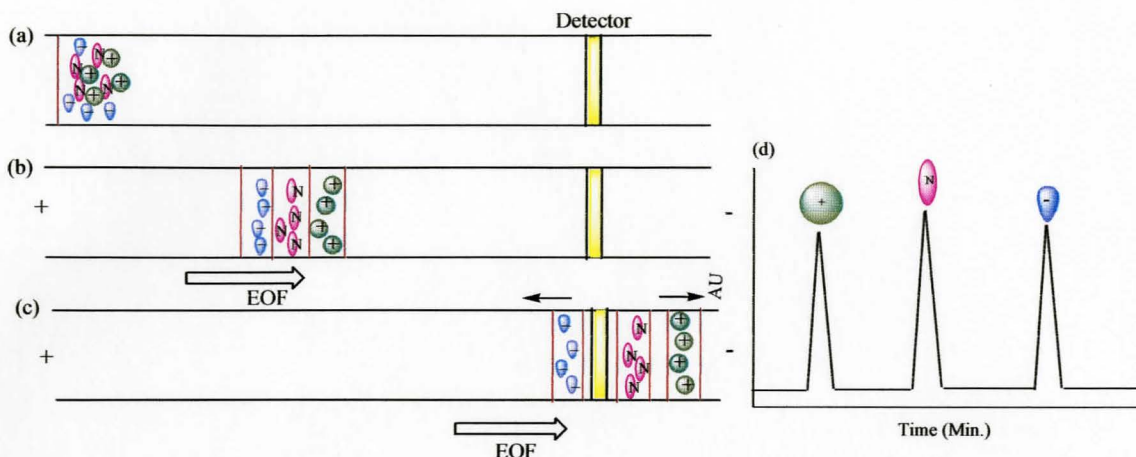


**Fig. 1.4** Schematic showing separation of a mixture of analytes based on their effective charge by CE: (a) sample injection, (b) zonal separation, (c) on-line detection and (d) electropherogram.

**1.4 (b).** **Fig. 1.4 (c)** shows that zonal separation of analytes continues until the EOF transports all species across a fixed detector window located at the cathodic end of the capillary. The monitoring of the absorbance signal as a function of time during electromigration generates an electropherogram, where the apparent analyte migration time is reflected by the superimposition of EOF and  $\mu_{ep, A}$ . The analyte mobility ( $\text{cm}^2 \text{V}^{-1} \text{s}^{-1}$ ),  $\mu_{ep, A}$  can be calculated from the apparent migration time in an electropherogram by re-arranging eq. 3 to the following equation:

$$\mu_{ep, A} = \frac{L_c L_d}{V} \left( \frac{1}{t_A} - \frac{1}{t_{eo}} \right) \quad (4)$$

where,  $L_c$  is the total capillary length,  $L_d$  is the effective capillary length to detector,  $V$  is the applied voltage,  $t_A$  is the apparent analyte migration time and  $t_{eo}$  is the migration time of a neutral EOF marker. Due to EOF variation, the measured migration times in CE typically have larger relative error ( $\text{CV} > 5\%$ ) than HPLC, however this can be

minimized by appropriate capillary pre-rinsing and storage techniques, as well as using internal standards. With the use of a neutral EOF marker (*e.g.*, 0.5% acetonitrile), the  $\mu_{ep, A}$  can be measured very precisely (CV < 1%) using commercial CE instruments with thermostatic control. Thus, most separation scientists prefer to consider  $\mu_{ep, A}$  rather than migration times as a reliable parameter to characterize CE separations.

## 1.2 Dynamic complexation using additives in CE

CE is a high resolution microseparation technique for charged analytes, but it is normally not applicable to resolve neutral analytes, which co-migrate as a single peak with the EOF. However, neutral analytes can be separated by CE either by off-line covalent derivatization with a charged reactant [15] or more conveniently via the addition of charged additives in the run buffer that form specific non-covalent interactions with analyte(s) of interest. The latter approach is advantageous since dynamic complexation occurs during electromigration directly in-capillary without off-line sample pretreatment, using single or multiple additives simultaneously. For instance, additives ranging from ionic surfactants [16], charged cyclodextrin derivatives [17] to monoclonal antibody receptors [18] can be used to resolve analyte mixtures with high selectivity in CE based on differential partitioning, inclusion complexation and affinity binding, respectively. In essence, the separation in CE is influenced by both electrokinetic (*e.g.*, mobility) and thermodynamic (*e.g.*, equilibria) parameters, which greatly enhances the resolution required for complex analyte mixtures. Unlike chromatography that uses a fixed amount of immobilized stationary phase in a column, separation optimization in CE can use

variable concentrations of additive(s) in free solution. This property is particularly important for tuning separation resolution using low amounts of additives, as well as modeling non-covalent interactions in CE without the requirement of solid-phase chemistry for immobilization that can alter ligand binding.

### 1.2.1 SDS micelles

Two of the most widely used additives in CE separations are sodium dodecyl sulphate (SDS) micelles and  $\beta$ -cyclodextrin ( $\beta$ -CD) macrocycles that are often employed in neutral and enantiomeric analyte separations, respectively. For example, neutral analytes can be separated in CE by the addition of SDS micelles in the run buffer via dynamic partitioning during electromigration. Micelles are dynamic molecular aggregates of surfactant monomers into which analytes can partition based on hydrophobic and electrostatic interactions. Above the critical micelle concentration (cmc), SDS surfactant monomers spontaneously aggregate to form spherical micelles comprising about 60 discrete surfactant species. Due to the large negative mobility of SDS micelles, the partition of neutral analytes during electromigration results in the formation of a charged complex. In CE, micelles are often referred to as “pseudo-stationary phases” since they represent an electrokinetically mobile apolar phase in free solution. In MEKC, the fraction of complex formed is directly related to the retention factor ( $k'$ ), which is dependent on the partition coefficient and concentration of micelle ( $k' = K[C]$ ), as described in the following equation based on 1:1 partitioning stoichiometry:

$$v\mu_{ep}^A = \frac{k'}{1 + k'} \mu_{ep,mc} \quad (5)$$

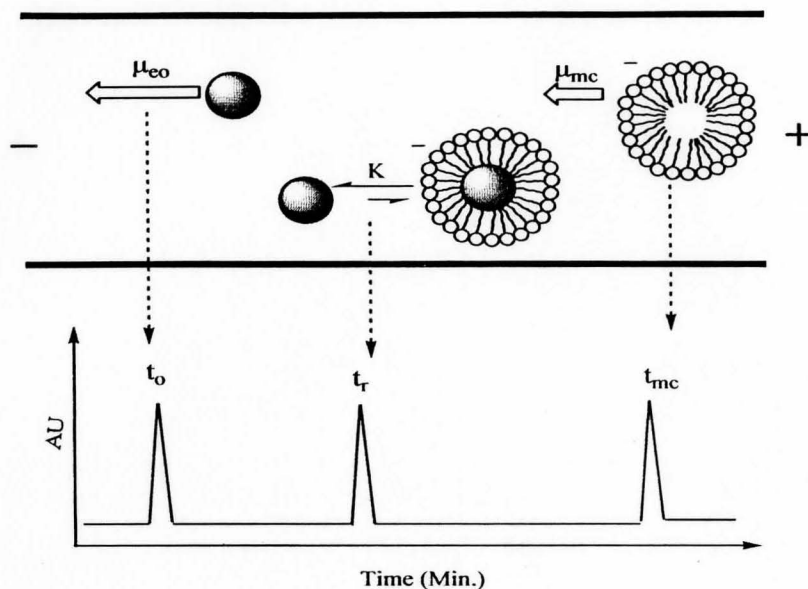


Fig. 1.5 Schematic of dynamic partitioning of neutral analytes using SDS as an additive in MEKC.

where,  $v$  is the viscosity correction factor,  $\mu_{ep}^A$  is the apparent mobility of a neutral species and  $\mu_{ep, mc}$  is the mobility of the micelle, which assumes negligible changes in micellar hydrodynamic size (*i.e.*, mobility) upon partitioning with a small analyte. In general, neutral analytes with stronger partitioning into SDS micelles have large apparent negative mobility shifts and thus longer migration times, as shown in **Fig. 1.5**. Similar to reverse-phase HPLC, the EOF marker or the migration time of an unretained species (void time) is given by  $t_o$  and the micelle migration time is given by  $t_{mc}$ , which is often measured by using a hydrophobic micellar marker, such as the dye Sudan IV [19]. Thus, neutral analytes that differentially partition with SDS typically have a migration times ( $t_A$ ) between  $t_o$  and  $t_{mc}$ . Separation optimization of analyte mixtures in MEKC is based on differences in  $k'$ , which is often modified by changes in micelle concentration, buffer pH and organic solvent content in aqueous solution.

### 1.2.2 Cyclodextrins

Cyclodextrins (CDs) are cyclic oligosaccharides synthesized by the enzymatic degradation of starch using the enzymes glycosyltransferase or cyclodextrinase, which are subsequently purified by chromatography and re-crystallization [20]. In contrast to micelles, CDs represent discrete and stable macrocycles with a defined structure. Moreover, CDs are intrinsically chiral and thus are widely used as chiral selectors for enantiomeric separations. For example,  $\beta$ -CD is composed of seven  $\alpha$ -1, 4 linked *D*-glucose residues that form a truncated cone macrocycle with a hydrophobic core and two hydrophilic rims consisting of asymmetric 1° and 2° hydroxyl moieties, as shown in Fig. 1.6. CDs are capable of forming host-guest inclusion complexes with a variety of small molecules. CDs are widely used in chromatographic and electrophoretic separations for chiral and achiral analytes, as well as in drug delivery for improving the solubility of water-insoluble compounds. Similar to MEKC, CDs and their derivatives can be used as additives in CE for improved resolution of charged enantiomers by dynamic inclusion complexation during electromigration [21]. However, since native CDs are neutral and co-migrate with the EOF, they are not applicable for resolving neutral analytes in CE since there is no net change in mobility upon complexation. In the case of charged analytes that undergo 1:1 dynamic complexation with a neutral CD, the apparent analyte mobility ( $\mu_{ep}^A$ ) can be described by the following equation:

$$v\mu_{ep}^A = \frac{1}{1 + K_B[C]} \mu_{ep,A} + \frac{K_B[C]}{1 + K_B[C]} \mu_{ep,AC} \quad (6)$$

where,  $v$  is the viscosity correction factor,  $K_B$  is the apparent binding constant,  $\mu_{ep,A}$  is

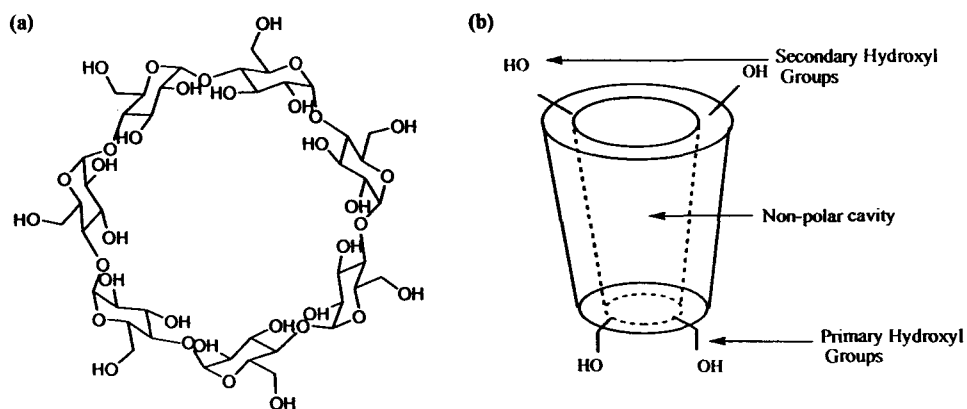


**Fig. 1.6** (a) Chemical structure of  $\beta$ -CD and (b) schematic of the truncated cone structure of the oligosaccharide macrocycle

the free analyte mobility of a charged solute and  $\mu_{ep, AC}$  is the mobility of the host-guest complex. In contrast to SDS micellar partitioning in MEKC, analyte inclusion complexation with a neutral CD results in a lower apparent mobility and shorter migration times as an increasing fraction of complex (reflected by second term of eq. 6) is formed at higher CD concentrations. Thus, the separation involving a neutral receptor with charged substrates in CE is based on three fundamental parameters [22], namely one thermodynamic factor,  $K_B$  and two electrokinetic parameters,  $\mu_{ep, A}$  and  $\mu_{ep, AC}$ . The importance of differences in  $\mu_{ep, AC}$  as a result of subtle differences in complex conformation involving chemically-similar guests will represent a major theme in the thesis. Although a variety of ionic CD derivatives are commercially available, the majority consist of heterogeneous mixtures of different degrees of substitution due to the similar reactivity of multiple hydroxyl moieties in the structure. Thus, alternative macrocycles with discrete and tunable chemical structural properties that have good water solubility, high purity and large intrinsic mobility properties are needed for

efficient separation of neutral analytes that is complementary to both SDS and CD additives in CE.

### **1.3 Calixarenes and resorcinarene macrocycles**

Calixarenes are metacyclophanes [23] that acquired their name because of the resemblance of the shape of one of the conformers to a Greek vase or “calix”, whereas “arene” indicates that it is an aromatic based macrocycle. The name was initially chosen to apply specifically to the phenol-derived cyclic oligomers, but it has subsequently taken on a more generic aspect and is now applied to a wide variety of structurally related compounds. The calixarene family can be divided into two major classes: (a) phenol-derived and (b) resorcinol-derived macrocycles, as illustrated in Fig. 1.7. Although larger cyclic oligomers can be isolated kinetically [23], the majority of studies have examined the thermodynamically stable calix[4]arene tetramers. In this thesis, the synthesis, characterization and selectivity of a water-soluble resorcin[4]arene derivative will be examined quantitatively by CE in aqueous solution based on a charged host-neutral guest model system. Relative to phenol-derived calixarenes, resorcin[4]arenes have electron-rich aromatic cavities with eight extra-annular phenolic hydroxyl moieties around the rim of the cavity (*i.e.*, octol) that can form a relatively stable macrocyclic structure based on hydrogen-bonding between adjacent resorcinol residues.

#### **1.3.1 Historical perspective**

Resorcinarenes have a long and noteworthy history in the field of supramolecular chemistry. In 1872, Baeyer [24] first reported that the acid-catalyzed condensation of

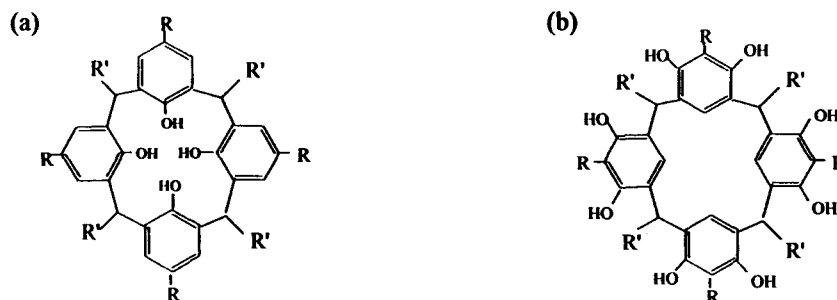


Fig. 1.7 Chemical structure of (a) phenol-derived and (b) resorcinol-derived calix[4]arenes.

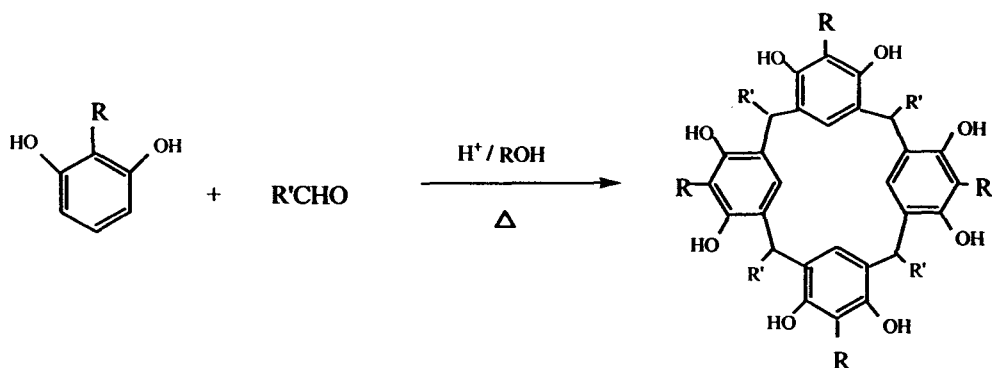
resorcinol with aldehydes, such as benzaldehyde or acetaldehyde generated unique crystalline and high melting compounds. The reaction was later investigated a decade later by Michael [25], who succeeded in isolating a pair of crystalline materials for which he postulated a cyclic dimeric structure. Similar experiments were carried out in subsequent years [26, 27], however the compounds remained relatively unnoticed until 1940, when Neiderl and Vogel [28] re-examined their chemistry. It was concluded on the basis of molecular weight determination that the resorcinol condensation products were best represented as cyclic tetramers, otherwise referred to as “Neiderl octols” or simply “octols”, which was later confirmed by X-ray crystallography [29]. In 1951 Cram and Steinberg [30] classified these compounds as  $[1_n]$ metacyclophanes, whereas Gutsche [31] later coined the name “calixarene” in 1975, although it did not appear regularly in literature until 1978. Despite the different usage of nomenclature in the literature, the term resorcin[4]arene will be used throughout this thesis.

### 1.3.2 Resorcin[4]arenes: Resorcinol-derived calixarenes

Resorcin[4]arenes are synthesized via an acid-catalysed reaction involving an

electron-rich resorcinol derivative (*e.g.*, 1,3-dihydroxybenzene, 1,3-dihydroxytoluene or 1,2,3-trihydroxybenzene) with a variety of substituted aldehydes. Note that the substituent at 2-position of the resorcinol modifies the extra-annular outer “rim” structure, whereas the substituent introduced by the aldehyde provides the functionality of the pendant “feet” position of the macrocycle. These positions serve as useful moieties for building larger and more extended supramolecular structures based on resorcin[4]arenes [24]. In general, the substituent introduced by the aldehyde at the methylene bridge is indicated by a prefix ‘C-substituent.’ For example, the resorcinol-derived compound from *p*-bromobenzaldehyde with resorcinol is referred to as *C-p*-bromophenyl resorcin[4]arene.

The general reaction of the acid-catalysed condensation reaction of a substituted aldehyde with resorcinol for the synthesis of resorcin[4]arenes is depicted in **Scheme 1.1**. Reactions are generally performed under reflux in methanol solvent under acidic conditions for over 12 hrs. Konishi *et. al.* [32] reported that during reaction higher order cyclic pentamers and cyclic hexamers are initially formed but upon completion of the reaction the major cyclic oligomer is the thermodynamically stable tetramer. Moreover, if the reaction is stopped before its completion, resorcin[5]arene and resorcin[6]arene macrocycles can be kinetically isolated. The yields of these larger cyclic oligomers are dependent on reaction conditions such as temperature and time. Resorcinarenes are commonly used to build larger and more rigid structures based on the bridging of adjacent phenolic moieties to form cavitands or carceplexes [33].



**Scheme 1.1** General reaction of the acid-catalyzed condensation of resorcinol with an aldehyde. Note that substituents on the resorcinol and aldehyde can provide a variety of different resorcin[4]arene derivatives.

### 1.3.3 Stereochemical properties of resorcin[4]arenes

Resorcin[4]arenes possess four prochiral centres at their methylene-bridged position and thus are capable of existing in four distinct diastereomeric configurations [34]. As a way to show the relationship between the prochiral centres, the macrocycle ring can be considered to be planar with respect to the residues R of the CHR-bridges pointing to one or the other side. Assigning one of the residues as a reference group (r) on the prochiral centre and then proceeding around the ring in a sequential clockwise progression, the residues of the other prochiral centres can be termed as cis (c) or trans (t) with respect to the reference group (r). The stereochemical relationships among the four R groups at the methylene bridges of resorcin[4]arenes are shown in **Fig. 1.8**. Since resorcin[4]arenes are not planar structures, they have the potential of existing in a variety of 3D conformations. Several different conformations of resorcin[4]arenes have been identified in solution [34], which are depicted in **Fig. 1.9**. The major conformations in which all four R feet are axially orientated include the crown and boat conformers, which are

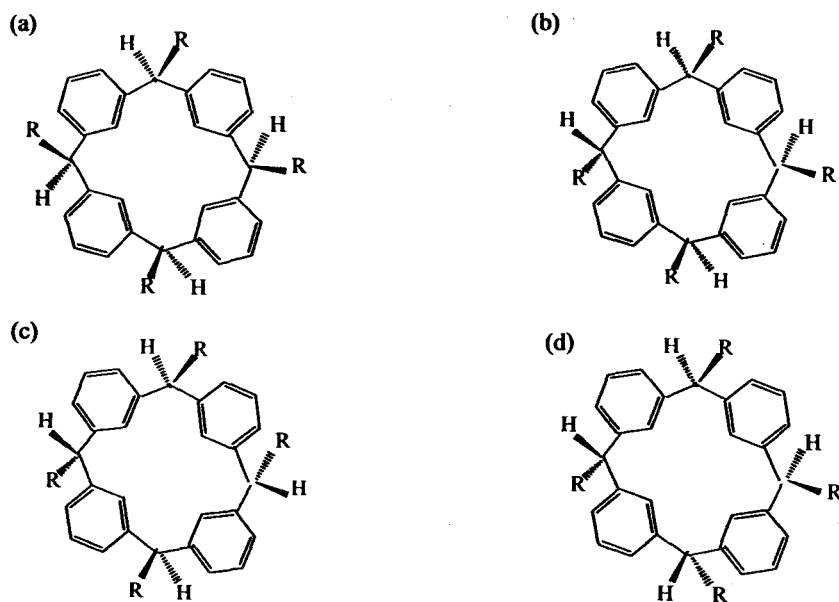


Fig. 1.8 Four diastereomeric configurations of resorcin[4]arenes: (a) rccc, (b) rect, (c) rtct and (d) rctt



Fig. 1.9 Two major conformations of resorcin[4]arenes: (a) crown and (b) boat conformers

equivalent to the “rccc” configuration. The bowl-shaped crown conformer with  $C_{4v}$  symmetry is the major thermodynamically stable product that has been most widely examined, and it can be isolated in the presence of other conformers of different solubility by repeated re-crystallization. Characterization of the fraction of different resorcin[4]arene conformers in a crude mixture can be readily assessed by  $^1\text{H-NMR}$ ,

since distereomeric proton resonances will have distinct chemical shifts due their unique chemical environments. As will be demonstrated later in the thesis, CE can also be used as a complementary technique to characterize the purity of charged resorcin[4]arene derivatives since each conformer will have a unique mobility based on differences in its hydrodynamic shape.

#### **1.4 Non-covalent interactions**

Host-guest inclusion complexation represents an important example of non-covalent interactions in nature, which is exemplified by the high affinity and selectivity of enzyme-substrate binding. Resorcin[4]arenes have been used as synthetic receptors to better understand the fundamental properties of non-covalent interaction in solution. Due to their unique chemical and structural properties, resorcin[4]arene inclusion complexation with small guests is controlled by both steric and specific non-covalent interactions, such as electrostatic, ion-dipole, dispersion, CH- $\pi$ / $\pi$ - $\pi$  and hydrogen bonding. Non-covalent interactions were first recognized by J. D. van der Waals in 1873 [35]. The structures of liquids, molecular aggregation, solvation phenomena, molecular crystals and the conformations of biopolymers, such as DNA and proteins are only a few phenomena dependent on non-covalent interactions. In contrast to covalent chemical bonding, non-covalent interactions are observed to act over distances of several angstroms or even tens of angstroms. The driving force for the mutual attraction between interacting molecules (*e.g.*, host-guest) is based on the intrinsic chemical and electronic properties of the molecules. Non-covalent interactions originate from interaction

between permanent multipoles, as well as between a permanent multipoles and induced multipoles. The respective energy terms, such as induction and dispersion are essentially attractive. However, the electrostatic term, depending on the orientation of the molecules, can be attractive or repulsive. The repulsive term, called exchange repulsion, is connected with overlap of occupied orbitals and prevents molecules from approaching too closely.

In many cases, a stable host-guest complex can only be realized when there is an additive contribution of multiple non-covalent interactions simultaneously. When steric factors and non-covalent interactions are highly complementary and directional, the binding process can be extremely selective, as in the case of the mutual recognition of DNA base pairs, primarily by hydrogen bonding, which has served as a motif in the design of many synthetic hosts capable of binding guests according to the same principles [36, 37]. Thus, the ability to tune the size, shape and chemical properties (*e.g.*, functional groups) of the host to minimize steric repulsion and maximize the interaction energy based on multiple non-covalent interactions with a specific guest serves to enhance the selectivity of molecular recognition. Non-covalent interactions are individually weak, but collectively can become very significant relative to covalent chemical bonds. A comparison of bond strengths of several different non-covalent interactions [38] is highlighted in **Table 1.1**.

#### **1.4.1 Ionic interactions**

The electrostatic energy that exists between oppositely charged ions is based on Coulombic attraction which is one of the strongest long-range types of non-covalent

**Table 1.1 Bond strengths involved in covalent and various non-covalent interactions**

<b>Bond Type</b>	<b>Bond Strength</b>	
	(kcal/mole)	(kJ/mole)
Covalent	> 50	> 210
Non-covalent		
- Ionic interactions	1-20	4-80
- Hydrogen bonding	3-7	12-30
- Hydrophobic interactions	< 1-3	3-12
- Dispersion forces	< 1-2.7	0.3-9

interactions as it is directly proportional to the charges of the ions and inversely proportional to the distance between ions as described by the following equation:

$$E = \frac{q_1 q_2}{4\pi\epsilon_0 r} \quad (8)$$

where,  $q_1$  and  $q_2$  are the charge state of the ions,  $\epsilon_0$  constant is the vacuum permittivity and  $r$  is the distance between the ions. The charge on an ion can be considered of as the result of an atom gaining or losing electrons, which signifies that the charge can be expressed as a multiple of the charge of an electron,  $e$  ( $1.602 \times 10^{-19}$  C). Thus, for a singly charged negative ion the charge is  $-e$ , whereas a doubly charged positive ion the charge is  $+2e$ . Electrostatic interactions are significant for oppositely charged ions with multiple charge states in low ionic strength aqueous solutions in order to decrease the extent of electrostatic shielding by formation of a hydrated electric double layer.

#### 1.4.2 Hydrogen bonding

Hydrogen bonding occurs between molecules that have a permanent net dipole resulting from hydrogen being covalently bonded to electronegative atoms, such as fluorine, oxygen or nitrogen. For example, significant intermolecular hydrogen bonds

operate in several different solvents and weakly ionic acids and bases, such as water ( $\text{H}_2\text{O}$ ), ammonia ( $\text{NH}_3$ ), hydrogen fluoride ( $\text{HF}$ ), methanol ( $\text{CH}_3\text{OH}$ ) and acetic acid ( $\text{CH}_3\text{COOH}$ ). Hydrogen bonding is a stronger intermolecular force than either dispersion forces or dipole-dipole interactions, since the hydrogen nucleus is extremely small and electropositive, whereas fluorine, oxygen and nitrogen are very electronegative. Thus, the electrostatic term is contributed by dipole-dipole interactions, which gives hydrogen bonds their highly directional nature. **Fig. 1.10** depicts several different types of hydrogen bonding interaction [39].  $\text{D-H}\cdots\text{A}$  is formed between a hydrogen attached to an electronegative donor atom (D) and a neighboring acceptor atom (A). Hydrogen bonding is by far one of the most important types of non-covalent interactions in biological systems due to its inherent directionality.

#### **1.4.3 Dipole-dipole interactions: Dispersion forces**

A dipole can be represented as two charges, equal in magnitude but opposite in sign, at a fixed distance from one another. The positive end of one dipole interacts attractively with the negative end of another dipole and vice versa. Thus, at any given instant the electron density about an atom may be asymmetrically distributed thus giving rise to a transient dipole [40] as shown in **Fig. 1.11**. The transient dipole on one atom can induce a dipole on a neighboring atom by distorting the neighbor's electron cloud, thereby resulting in a temporary attractive interaction that reduces the energy of the system. It is important to note that these are not permanent dipoles, but are transient since the electron density is continuously fluctuating. The net result is an attractive interaction between two

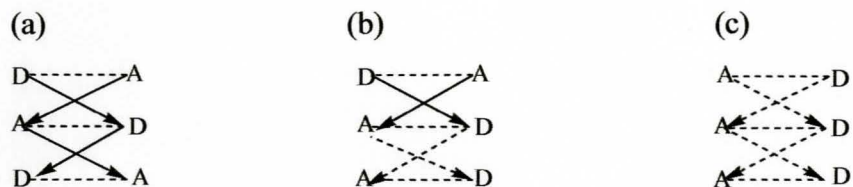


**Fig. 1.10** Three different types of hydrogen bonding interactions involving a donor (D) and acceptor (A).

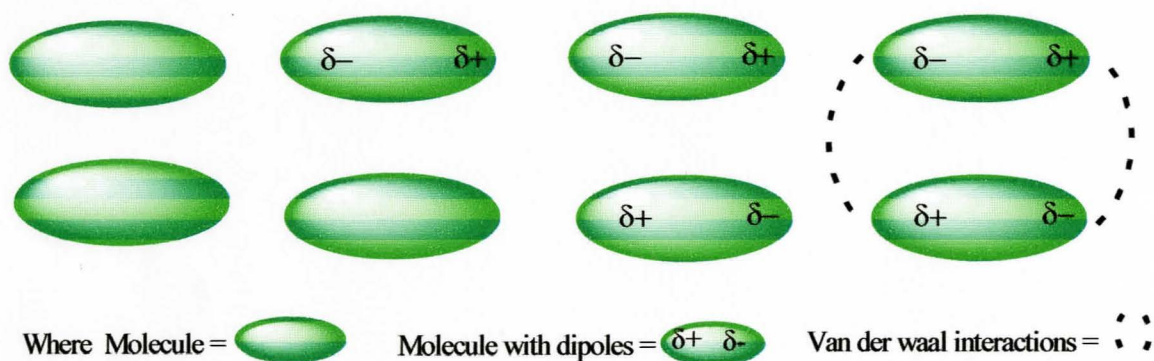


**Fig. 1.11** Schematic of transient dipole-induced dispersion interactions (Van der Waal) in two neutral molecules resulting in a net attractive force.

electrically neutral molecules at extremely close distances since the energy of interaction is inversely proportional to sixth power of distance. In small atoms, the electrons are held tightly by the nucleus and are not as readily polarized (distorted) as in larger atoms with electrons further from the nucleus. In general, the larger the molecule (total number of atoms) containing polarizable atoms, the greater is the magnitude of dispersion force.

#### 1.4.4 CH- $\pi$ interactions

The CH- $\pi$  is a weak type of hydrogen bonding that occurs specifically between CH groups (often -CH<sub>3</sub>) and electron rich-aromatic systems. CH groups are referred to as soft

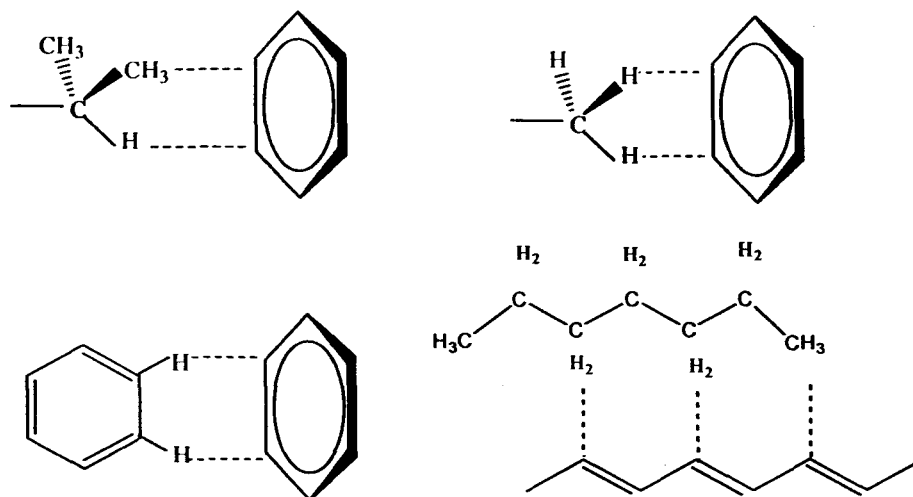


Fig. 1.12 Schematic of several different types of CH- $\pi$  interactions

acids, whereas  $\pi$ -systems are referred to as soft bases [41]. The CH- $\pi$  interaction is characteristic of a relatively large contribution from delocalization (charge transfer from  $\pi$  to  $\sigma^*$ ) and dispersive interaction as compared to the normal hydrogen bonding [42]. A unique feature of CH- $\pi$  interactions is that it can play a role in polar as well as non-polar media, unlike hydrogen bonding. Groups which may be involved in the CH- $\pi$  interaction include methyl, isopropyl and long chain alkyl groups in conjunction with unsaturated conjugated bonds and aromatic moieties. Fig.1.12 depicts two examples of CH- $\pi$  interaction, whose magnitude is determined by the relative orientation of the molecules, as well as the number of CH donor atoms and the electron density of the conjugated system. CH- $\pi$  interactions can play a very important role in inclusion complexation involving resorcin[4]arenes given their electron-rich aromatic core cavity.

#### 1.4.5 Hydrophobic interactions

In aqueous solutions, hydrophobic interactions or the “hydrophobic effect” is often a

major driving force in host-guest inclusion complexation and protein folding [43]. Hydrophobic interactions describe the tendency of non-polar, water-insoluble groups (especially hydrocarbons) to spontaneously associate in aqueous solutions. This association is frequently accompanied by little change of enthalpy ( $\Delta H \approx 0$ ) due to dispersion interactions, and it is most often associated with favorable entropy change ( $\Delta S > 0$ ). In many cases, molecular association/aggregation caused by hydrophobic interactions is related to the entropy increase with release of bound water [44].

#### 1.4.6 $\pi - \pi$ interactions

Non-covalent interactions between  $\pi$ -systems have been recognized for over half a century. Aromatic-aromatic or  $\pi$ - $\pi$  interactions are important non-covalent intermolecular forces similar to hydrogen bonding. They control such diverse phenomena as the vertical base-base stacking which stabilize the double helical structure of DNA [45], the intercalation of drugs into DNA [46], the tertiary structures of proteins [47], and the complexation in many host-guest systems [48]. Sanders *et al.* [49] highlighted that  $\pi$ - $\pi$  interactions are not due to an attractive electronic interaction between two  $\pi$ -systems, but rather occur when the attractive interactions between  $\pi$ -electrons and a  $\sigma$ -framework outweigh unfavorable contributions such as  $\pi$ -electron repulsion. Since the C-H bond generally has a small dipole moment, an attraction exists between the positively polarized hydrogen atom(s) and negatively charged  $\pi$ -face of the aromatic system. Three major types of  $\pi$ - $\pi$  interactions have been classified based on their relative orientations, including T-shaped, face-to-face and offset conformations as depicted in Fig. 1.13. In fact, the T-shaped conformation can also be considered a type of

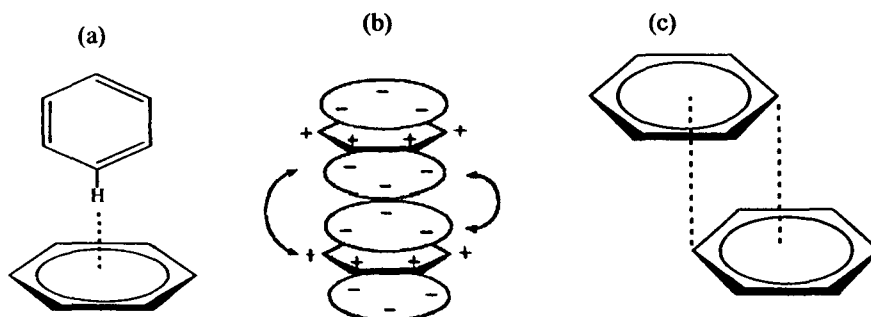


**Fig. 1.13** Schematic of three major types of CH- $\pi$  and  $\pi$ - $\pi$  interactions involving aromatic systems figures in one figure (a) T-shaped , (b) face to face and (c) offset conformation

CH- $\pi$  interaction. It is important to note that  $\pi$ -stacking does not necessarily have to be a symmetrical face-to-face orientation, but can also be an offset or slipped packing.  $\pi$ - $\pi$  interactions is a commonly used motif found in nature for stacking aromatic moieties with approximately parallel molecular planes separated by interplanar distances of about 3.3–3.8 Å [50]. Substituents or heteroatoms on the aromatic ring alter the uniform charge distribution in the conjugated system, which can significantly influence the magnitude of  $\pi$ - $\pi$  interactions. For instance, in the case of face-to-face  $\pi$  stacking, the most stable combination is when both partners are electron-poor, whereas electron donating substituents weaken a  $\pi$ - $\pi$  interaction due to excessive electronic repulsion [51]. In general, the order of stability in the interaction of two  $\pi$  systems is  $\pi$ -deficient- $\pi$ -deficient >  $\pi$ -deficient- $\pi$ -rich >  $\pi$ -rich- $\pi$ -rich.

## 1.5 Research objectives

The major focus of this thesis is to examine non-covalent interactions involving a charged host-neutral guest model system by CE, in conjunction with NMR and computer

modeling. The inclusion complexation of a group of neutral corticosteroids with an anionic resorcin[4]arene derivative is studied in aqueous buffered solution. Noteworthy, this research represents the first example of using a macrocycle/receptor as both an electrokinetic host and intrinsic buffer for enhanced molecular recognition of corticosteroids. The research highlights that CE can be used a unique platform to exploit differential binding affinity (thermodynamic) and conformational (electrokinetic) properties of the host-guest complex for improved selectivity relative to conventional methods. Improved affinity and size selectivity for neutral corticosteroid guests was achieved when using an resorcin[4]arene as an intrinsic buffer in CE by reducing the influence of extrinsic electrolytes. Five specific research objectives will be addressed in this thesis:

1. Synthesis and purification of a water-soluble *C*-tetraethylsulphonate methyl-resorcin[4]arene derivative (TESMR)
2. Characterization of the spectroscopic, weak acidity and intrinsic buffer capacity properties of TESMR
3. Quantitative assessment of the binding interactions of TESMR with a group of model neutral corticosteroids
4. Determination of the driving force of TESMR-corticosteroid interaction in aqueous solution and the influence of electrolyte composition.
5. Enhancing the selectivity of molecular recognition via coupling of thermodynamic and electrokinetic parameters associated with complex formation.

## 1.6 References

- [1] Dovichi, N. J.; Zhang, J., *Angew. Chem. Int. Ed.* **2000**, 39, 4463-4467.
- [2] Michaelis, L., *Invertin, Biochem. Z.* **1909**, 16, 81.
- [3] Vesterberg, O., *Acta Chem. Scand.* **1969**, 23, 2653.
- [4] Dale, G., and; Latner, A. L., *Clin. Chem. Acta* **1969**, 24, 61.
- [5] Macko, V., Stegemann, H., *Z. Physiol. Chem.* **1969**, 350, 917.
- [6] Stegemann, H., *Angew. Chem. Int. Ed.* **1970**, 9, 643.
- [7] Jorgenson, J. W., and Lukas, K.D., *Anal. Chem.* **1981**, 53, 1298.
- [8] Terabe, S.; Otsuka, K.; Ichikawa, K.; Tsuchiya, A.; Ando, T., *Anal. Chem.* **1984**, 56, 111-113
- [9] Terabe, S.; Otsuka, K.; Ando, T., *Anal. Chem.* **1985**, 57, 834-841
- [10] Landers, J. P., "Handbook of Capillary Electrophoresis" Boca Raton: CRC press, USA; **1997**.
- [11] Wang, D.; Yang, G.; Song, X., *Electrophoresis* **2001**, 22, 464-469.
- [12] Gluck, S. J.; Cleveland, J. A., *J. Chromatogr. A* **1994**, 680, 49-56.
- [13] Muijeselaar, P. G.; van Straten, M. A.; Claessens, H. A.; Cramers, C. A., *J. Chromatogr. A* **1997**, 766, 187-195.
- [14] Britz-McKibbin, P.; Chen, D. D. Y., *Electrophoresis* **2002**, 23, 880-888.
- [15] Evangelista, R. A.; Liu, M.; Chen, F. A., *Anal. Chem.* **1995**, 67, 2239-2245.
- [16] Oudhoff, K. A.; van Damme, F. A.; Mes, E. P. C.; Schoenmakers, P.; Kok, W. T., *J. Chromatogr. A* **2004**, 1046, 263-269.
- [17] Pak, C.; Marriott, P. J.; Carpenter, P. D.; Amiet, R. G., *J. Chromatogr. A* **1998**, 793,

357-364.

[18] Okun, M. V.; Moser, R.; Blaas, D.; Kenndler, E., *Anal. Chem.* **2001**, 73, 3900-3906.

[19] Ackermans, M. T.; Everaerts, F. M.; Beckers, J. L., *J. Chromatogr.* **1991**, 585, 123-131.

[20] Fanali, S., *J. Chromatogr. A* **2000**, 875, 89-122.

[21] Nevado, B. J. J.; Cabanillas, G. C.; Llerena, V. J. M.; Robledo, R. V., *J. Chromatogr. A* **2005**, 1072, 249-257.

[22] Britz-McKibbin, P.; Chen, D. D. Y., *J. Chromatogr. A* **1997**, 781, 23-34.

[23] Gutsche, C. D., "Calixarenes" Royal Society of Chemistry: Cambridge;. **1989**.

[24] Gutsche, C. D., "Calixarenes Revisited" Royal Society of Chemistry: Cambridge; **1989**.

[25] Michael, A., *J. Amer. Chem. Soc.* **1883**, 5, 338.

[26] Mohlau, R., and Koch, P., *Ber.* **1894**, 27, 2887.

[27] Liebermann, C.; Lindenbaum, S., *Ber.* **1904**, 37, 1171.

[28] Neiderl, J. B.; Vogel, H. J., *J. Amer. Chem. Soc.* **1940**, 62, 2512.

[29] Erdtman, H.; Hogberg, S.; Abrahamsson, S.; Nilsson, B., *Tetrahedron Lett.* **1968**, 9, 1679-1682.

[30] Cram, D. J.; Steinberg, H., *J. Amer. Chem. Soc.* **1951**, 73, 5691.

[31] Gutsche, C. D.; Muthukrishnan, R., *J. Org. Chem.* **1978**, 43, 4905.

[32] Konishi, H.; Nakamura, T.; Ohata, K.; Kobayashi, K.; Morikawa, O., *Tetrahedron Lett.* **1996**, 41, 7383-7386.

[33] Cram, D. J.; Karbach, S.; Moran, J. R., *J. Amer. Chem. Soc.* **1982**, 104, 5826-5828.

- [34] Asfari, Z.; Bohmer, V.; Harrowfield, J.; Vicens, J., "Calixarenes 2001"; Kluwer Academic Publishers, The Netherlands. 2001.
- [35] van der Waals, J. D., Doctoral Dissertation, Leiden. 1873.
- [36] Conn, M. M.; Deslongchamps, G.; de Mendoza, J.; Rebek, J. J., *J. Amer. Chem. Soc.* 1993, 115, 3548-3557.
- [37] Blake, J. F.; Jorgenson, W. L., *J. Amer. Chem. Soc.* 1990, 112, 7269-7278.
- [38] <http://www.hsc.wvu.edu/som/bmp/files/shiemke/BCH531Lect2.ppt>
- [39] Brunsveld, L.; Folmer, B. J. B.; Meijer, E. W.; Sijbesma, R. P., *Chem. Rev.* 2001, 101, 4071-4097.
- [40] Chang, H., "Chemistry Annotated Instructor's Edition"; McGraw- Hill: New York, 2005.
- [41] Pearson, R. G.; Songstad, J., *J. Amer. Chem. Soc.* 1967, 89, 1827-1836.
- [42] Nishio, M.; Hirota, M.; Umezawa, Y., *Tetrahedron* 1995, 51, 8665-8701
- [43] Tanford, C., "The Hydrophobic Effect"; Wiley Interscience: New York, 1973.
- [44] Muller-Dethlefs, K.; Hobza, P., *Chem. Rev.* 2000, 100, 143-167
- [45] Saenger, W., "Principles of Nucleic Acid Structure"; Springer-Verlag: New York, 1984.
- [46] Wakelin, L. P. G., *Med. Res. Rev.* 1986, 6, 275-340.
- [47] Burley, S. K.; Petsko, G. A., *Adv. Protein Chem.* 1988, 39, 125-129.
- [48] Askew, B.; Ballester, P.; Buhr, C.; Jeong, K. S.; Jones, S.; Parris, K.; Williams, K.; Rebek, J. Jr, *J. Amer. Chem. Soc.* 1989, 111, 1082-1090.
- [49] Hunter, C. A.; Sanders, J. K. M., *J. Amer. Chem. Soc.* 1990, 112, 5525-5534.

[50] Janiak, C., *J. Chem. Soc. Dalton Trans.*, **2000**, 21, 3885-3896.

[51] Cozzi, F.; Siegel, J. S., *Pure Appl. Chem.* **1995**, 67, 683.

## CHAPTER 2

### Synthesis and Characterization of a Water-Soluble Resorcin[4]arene

#### Abstract

This chapter focuses on the synthesis, purification and characterization of an anionic tetrasulphonate derivative of 2-methyl resorcin[4]arene (TESMR). TESMR was synthesized by an acid-catalyzed condensation reaction of a protected aldehyde (*i.e.*, 1, 3-dioxane derivative) with 2-methyl resorcinol, where the all-cis crown conformer was isolated via repeated recrystallization. The purified single conformer of TESMR was then desalted by tangential flow fractionation in order to remove any residual low molecular weight salts prior to characterization. The characterization of TESMR was performed by several analytical techniques, namely  $^1\text{H}$  NMR, ESI-MS, UV absorbance, fluorescence and CE. The purity of TESMR was confirmed by  $^1\text{H}$  NMR experiments to be approximately 96 %. The weak acidity properties of TESMR (*i.e.*, phenolic protons) were also assessed by UV absorbance and CE. The measurement of the analyte mobility change as a function of pH (6-11) revealed that TESMR had three distinct  $\text{pK}_a$  values, namely  $\text{pK}_{a1} = (7.4 \pm 0.3)$ ,  $\text{pK}_{a2} = (9.1 \pm 0.3)$  and  $\text{pK}_{a3} = (9.9 \pm 0.3)$ . Due to its similarity to physiological neutral pH conditions, the buffer capacity of TESMR solutions at  $\text{pK}_{a1}$  were assessed by CE in comparison to conventional buffers, such as phosphate, which demonstrated that TESMR can be used as an intrinsic buffer and electrokinetic host with extremely stable pH and ion transport properties.

## 2.1 Introduction

As most biological processes in nature occur in water, it is important to develop water-soluble synthetic receptors to better understand fundamental non-covalent interactions influencing biomolecular interactions. Synthetic macrocycles have proved to be a useful model system to explore the dynamics of inclusion complexation as an analogy to substrate binding in an active site of an enzyme [1]. Extensive studies of cyclodextrins [2] and water-soluble cyclophanes [3] have demonstrated that steric and solvent-based hydrophobic effects are the major factors influencing inclusion complexation of apolar molecules in the cavity of these macrocycles. Depending on the chemical properties of the substrate (*e.g.*, charge, aromaticity), other types of non-covalent interactions can also play an important role, such as cation- $\pi$  [4],  $\pi$ - $\pi$  [5], and CH- $\pi$  [6]. The major motivation for studying water-soluble resorcin[4]arenes derivatives in this thesis is to understand ways to enhance the apparent binding affinity of inclusion complexation in aqueous solution using CE.

To date, the majority of resorcin[4]arenes reported in literature have had poor water-solubility properties and their complexation with small guests have been examined in apolar solvents. One way to enhance resorcin[4]arene water-solubility is to deprotonate most of the phenolic (*e.g.*, octol) protons under extremely alkaline pH conditions (pH > 11) [7]. However, this strategy drastically changes the structural properties of resorcin[4]arenes whose conformation is stabilized by H-bonding between adjacent phenolic moieties. Alternatively, resorcin[4]arenes can be derivatized with weakly ionic or strongly ionic functional groups either at the rim of the cavity by direct modification of

the 2-position (Type 1) or 1,3-phenolic moieties (Type 2) on the resorcinol, or more conveniently by substitution of the pendant “feet” group (Type 3) via appropriate choice of aldehyde reactant for acid-catalyzed condensation. The latter resorcin[4]arene derivative is preferred since it preserves the functional and structural integrity of the upper rim of the cavity which is important for analyte inclusion complexation and intrinsic buffer capacity, while still providing adequate water-solubility with minimal interference. There have been several different water-soluble resorcin[4]arene derivatives reported in the literature, including tetrasulfanatomethyl resorcin[4]arene [8] (Type1), resorcin[4]arene octacarboxylate [9] (Type 2) and TESMR [10] (Type 3), whose structures are depicted in Fig. 2.1. In general, the use of strongly acidic monoprotic (*e.g.*, sulphonic acids) derivatives of resorcin[4]arene are preferred relative to weakly acidic polyprotic groups (*e.g.*, carboxylic acid, phosphoric acid) since their charge is independent of  $\text{pH} > 4$ . Moreover, in the context of CE applications, anionic resorcin[4]arene derivatives are preferred since they have less tendency to adsorb irreversibly onto the silanol capillary surface unlike cationic derivatives. The intrinsic charge and high negative mobility of water-soluble resorcin[4]arene derivatives also plays a critical role in the separation mechanism of neutral guests by CE, as will be later discussed in chapter 3 of this thesis.

Recently, TESMR [11] was introduced as a new class of additive in CE due to its water solubility, high negative mobility and unique selectivity for positional nitrophenol isomers relative to an anionic cyclodextrin. Although TESMR was previously used to qualitatively resolve a mixture of neutral analytes for separation in CE, a quantitative

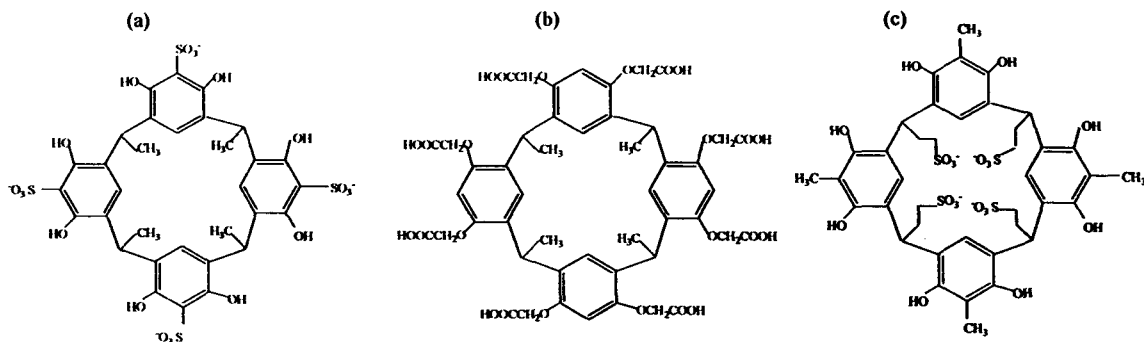


**Fig. 2.1** Three major types of water-soluble resorcin[4]arene derivatives including (a) Type 1, (b) Type 2 and (c) Type 3 based on the relative location of charged moiety.

study of inclusion complexation and understanding of the separation mechanism has not yet performed. The focus of this chapter is to thoroughly characterize TESMR that was synthesized in our laboratory using a variety of techniques, including  $^1\text{H-NMR}$ , CE, ESI-MS, UV absorbance and fluorescence spectroscopy. To the best of our knowledge, the weak acidity and intrinsic mobility properties of a water-soluble resorcin[4]arene have not been investigated to date. Our work demonstrated for the first time that a macrocycle can act as an intrinsic buffer and electrokinetic host with extremely stable pH and ion transport properties even at low ionic strength. These preliminary results were critical to subsequent work in chapter 3 of this thesis involving the quantitative study of the binding interaction of TESMR with a group of neutral corticosteroids.

## 2.2 Experimental

### 2.2.1 Chemicals

2-(2-bromoethyl)-1,3-dioxane, 2-methylresorcinol, deuterium oxide were purchased from Sigma-Aldrich Inc. (St. Louis, USA). Methanol was purchased from Caledon

Laboratories Ltd. (Georgetown, Canada), whereas concentrated HCl was obtained from BDH Inc. (Toronto, Canada). Sodium sulphite was purchased from Alfa Aesar (Ward Hill, USA) and anhydrous ethylether was obtained from Fisher Scientific Chemicals (New Jersey, USA). Ethyl alcohol anhydrous was purchased from Commercial Alcohols (Brampton, Canada). De-ionized water which used for all buffer and sample preparation was obtained using a Barnstead EASY pure II LF ultrapure water system (Dubuque, Iowa, USA). The background electrolyte buffers were prepared using dihydrogen sodium phosphate, sodium bicarbonate and sodium tetraborate decahydrate (borax). Dihydrogen sodium phosphate was purchased from Alfa-Aesar (Ward Hill, MA., USA) and sodium tetraborate decahydrate and sodium bicarbonate were obtained from Sigma-Aldrich (St.Louis, Mo., USA). The pH of the buffers was modified by using 0.1M NaOH to obtain the desired pH.

## **2.2.2 Apparatus and Procedure**

### **2.2.2.1 Synthesis of TESMR**

Tetraethylsulphonated derivative of 2-methyl resorcinol (TESMR) was synthesized via an acid-catalyzed condensation of sodium 2-formylethane-1-sulphonate with 2-methylresorcinol according to the method described by Aoyama *et al* [10]. A two-phase reaction of 2-(2-bromoethyl)-1-3-dioxane (10mmol) and an aqueous solution (10ml) of sodiumsulphite (20mmol) was stirred at 100°C for 24 hours under reflux. To the resultant homogeneous solution, water (10ml) was added and the mixture was washed with ether (20ml × 3) to extract unreacted bromo-alkyl-dioxane. To this mixture ethanol

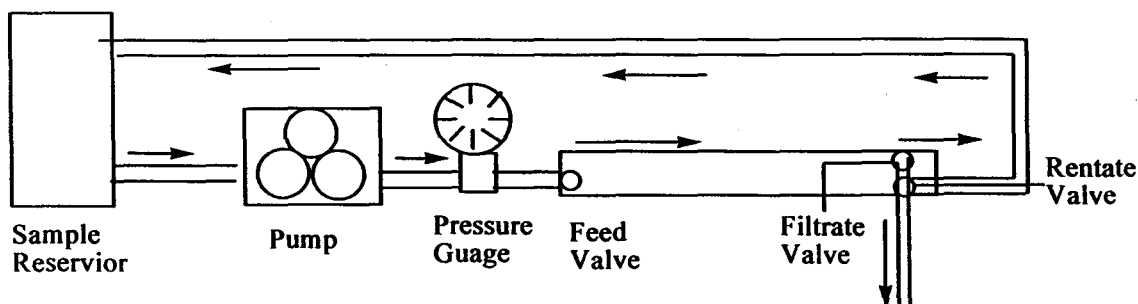


Fig. 2.2 Pictorial illustration of TFF that uses a porous 1000 Da MWCO filter for desalting.

(20mL), methylresorcinol (18mmol) and concentrated HCl (3 mL) were added and stirred at 100°C for 24 hours under reflux. The product was dried and purified by repeated recrystallization with methanol-water (50:50). The product was then desalted using TFF to remove inorganic salts. Desalted TESMR was dried using rotavap to produce orange coloured crystals whose elemental composition has been reported to be  $C_{40}H_{44}O_{20}S_4Na_4 \cdot 4H_2O$  [10].

#### 2.2.2.2 Purification and desalting

TESMR was purified and desalted using a tangential flow filtration (TFF) technique using a Masterflex® Console Drive (Cole-Parmer Instrument) equipped with a Masterflex® pump (Model No. 7021-20) and Masterflex® (06409-16 Tygon®) tubing was used. A minimate™ TFF capsule (Pall Corporation) with a 1000 Da MWCO (molecular weight cut-off) cartridge filter was used. System hold-up volume was measured to be about 13.5 mL. Cross flow rate at 30 mL/min. and the filtrate flow rate at 0.7 mL/min. were optimized at a trans membrane pressure of 12 psi. An illustration of TFF is shown in Fig. 2.2. Sample from the reservoir was fed onto the cartridge with a

built-in membrane of MWCO 1000 Da. The membrane acts as a sieve and filters out low molecular weight salts. The conductivity of the retentate was measured over time using a MC 126 conductivity meter (Mettler Toledo Inc.). TESMR was initially dried using a BÜCHI Rotavapor R-200 followed by vacuum drying overnight.

### ***2.2.2.3 Capillary electrophoresis***

An automated P/ACE System 2100 capillary electrophoresis system (Beckman-Coulter Canada, Inc.) equipped with a UV detector was used for TESMR purity assessment and determination of TESMR  $pK_a$ . All procedures were carried out using narrow fused-silica capillaries (Polymicro Technologies, Phoenix, USA.) with 50  $\mu\text{m}$  i.d. and 375  $\mu\text{m}$  o.d and 47 cm in total length. CE analysis of different purification stages of TESMR (*i.e.*, crude, 1<sup>st</sup> and 2<sup>nd</sup> recrystallization, TFF desalted product) were detected using a 214 nm narrow bandpass filter. CE studies were performed using 50 mM carbonate buffer, pH 9.5 at 25°C and a voltage of 25 kV for TESMR purity determination, whereas 50 mM phosphate and carbonate buffers ranging from pH 6.0-11.0. were used for TESMR  $pK_a$  determination.

### ***2.2.2.4 Characterization of TESMR***

Characterization of TESMR in D<sub>2</sub>O was performed using a 200 MHz NMR spectrometer. Electrospray ionization mass spectrometry (ESI-MS) was performed on a Micromass Quattro Ultima quadrupole instrument. ESI was operated using a negative ion mode with an applied voltage of +3 kV on the sprayer tip. N<sub>2</sub> was used as a nebulizing as

well as drying gas. The analyte carrier solution was methanol:water 50:50 and the flow rate was 10  $\mu\text{L}/\text{min}$ . 0.1 mM TESMR concentration was used in the sample.

#### **2.2.2.5 Spectroscopic measurements**

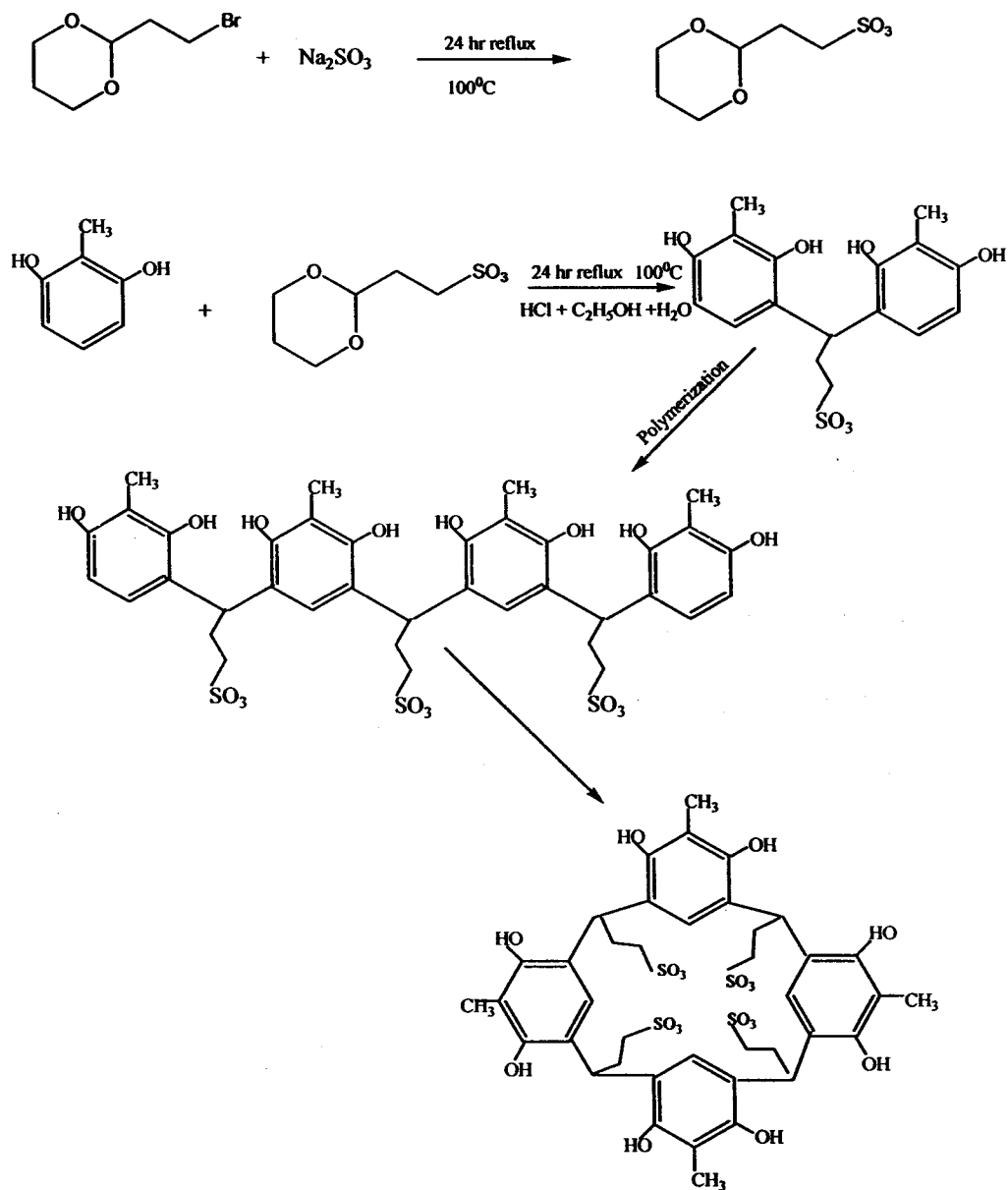
Fluorescence properties of TESMR were studied using Fluorolog ISA Jobin Yvon-spex Instruments S.A., Inc. UV 266 nm excitation was used and the emission scan range was from 285 nm to 500 nm using a slit width of 5 mm. The concentration of TESMR and tryptophan was 2  $\mu\text{M}$ . UV absorbance studies were conducted on Varian Cary 50 spectrophotometer using 20  $\mu\text{M}$  TESMR in 50 mM phosphate buffer from pH 6.0 to 8.5 with a wavelength range from 200-600 nm.

### **2.3 Results and Discussion**

#### **2.3.1 TESMR synthesis, purification and desalting**

TESMR was synthesized via an acid-catalysed condensation reaction of sodium 2-formylethane-1-sulfonate with 2-methyl resorcinol according to the method by Aoyama *et al.* [10]. The two-step chemical synthesis and reaction mechanism is illustrated in **Scheme 2.1**. The thermodynamically stable all-cis crown conformer of TESMR was purified by repeated recrystallization in MeOH:water, which was subsequently desalted by TFF. Desalting was important since TESMR will be used in CE binding studies in which Joule heating caused by excess mobile salts can result in band broadening and poor resolution, as well as influence apparent binding constant measurements.

**Scheme 2.1**



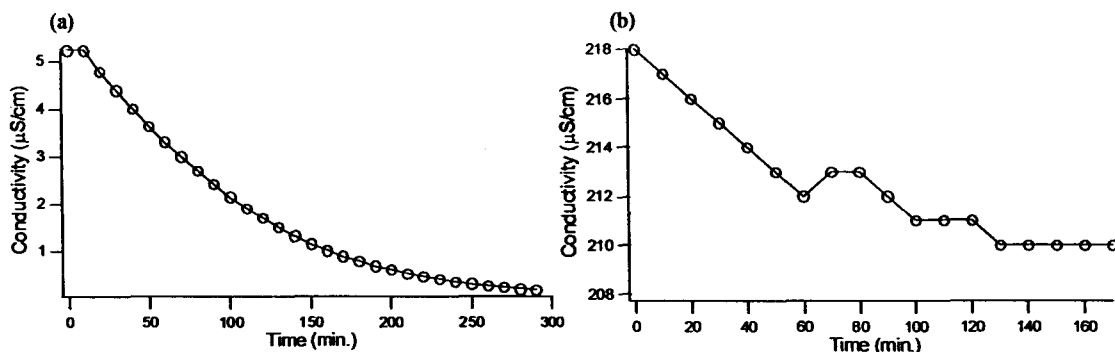


**Fig 2.3** (a) Measured conductivity as a function of TFF time using model 100mM NaCl solution and (b) measured conductivity as a function of TFF time using recrystallized TESMR product.

by TFF. Desalting was important since TESMR will be used in CE binding studies in which Joule heating caused by excess mobile salts can result in band broadening and poor resolution, as well as influence apparent binding constant measurements.

TFF is a rapid and efficient technique for purifying, desalting and concentrating large volumes of sample. The conductivity of the retentate was measured over time in order to establish when desalting had been completed. Optimization of TFF was first examined using 100 mM NaCl as a model solution and the conductivity ( $\mu\text{S}/\text{cm}$ ) of the retentate solution was measured over time as depicted in Fig. 2.3 (a). There was a significant decrease in conductivity after 4 hrs indicating that lower molecular weight conductive salts had been effectively removed in the filtrate. After initial TFF optimization, the technique was next applied for desalting of TESMR, as shown in Fig. 2.3 (b). It is evident that after 2 hours, the conductivity of the TESMR retentate solution remained constant indicating that desalting was complete. However, there was a high residual conductivity due to high concentrations of the charged TESMR macrocycle which is itself highly conductive.

### 2.3.2 TESMR characterization

Singlet aromatic 'H' and methyl 'H' NMR signals were consistent with the bowl-shaped conformer of TESMR [10]. Five proton resonances were observed for aromatic (CH) 6.796 ppm, methyl (CH<sub>3</sub>) 1.852 ppm, methylene (CH<sub>2</sub>) 2.382 ppm, methylene (CH<sub>2</sub>-SO<sub>3</sub>) 2.726 ppm and methine (CH-CH<sub>2</sub>) 4.505 ppm, which was assigned to the structure of TESMR as shown in Fig. 2.4 and Fig. 2.5. <sup>1</sup>H-NMR spectra of crude and desalted shows significant reduction of impurities at each TESMR purification stage. Table 2.1 summarizes the reduction of impurity peak '\*' to about 3.5 % relative to aromatic peak taken as 100 % based on relative peak integration using <sup>1</sup>H-NMR. It is apparent that TFF desalting was critical to significantly reducing the major impurity peak.

Purity assessment of TESMR was also performed by comparing different stages of TESMR namely, crude, 1<sup>st</sup> recrystallization, 2<sup>nd</sup> recrystallization and after TFF desalting in carbonate buffer using CE. It is evident in the electropherograms depicted in Fig. 2.6 that other isomeric TESMR conformational products with a high negative mobility are also present in the crude sample but are eliminated with repeated recrystallization resulting in purification of the *all-cis* bowl-shaped macrocycle conformer [12]. However, an unknown impurity (< 3.5 %, as estimated by <sup>1</sup>H-NMR relative peak integration) was observed in both NMR and CE data (co-migrating near the EOF) even after TFF desalting is suggestive of a low molecular weight weakly acidic aromatic precursor or side-product that has yet to be identified. However, the degree purification (> 96.5 %) of the desalted TESMR product was deemed sufficient to continue with subsequent studies.

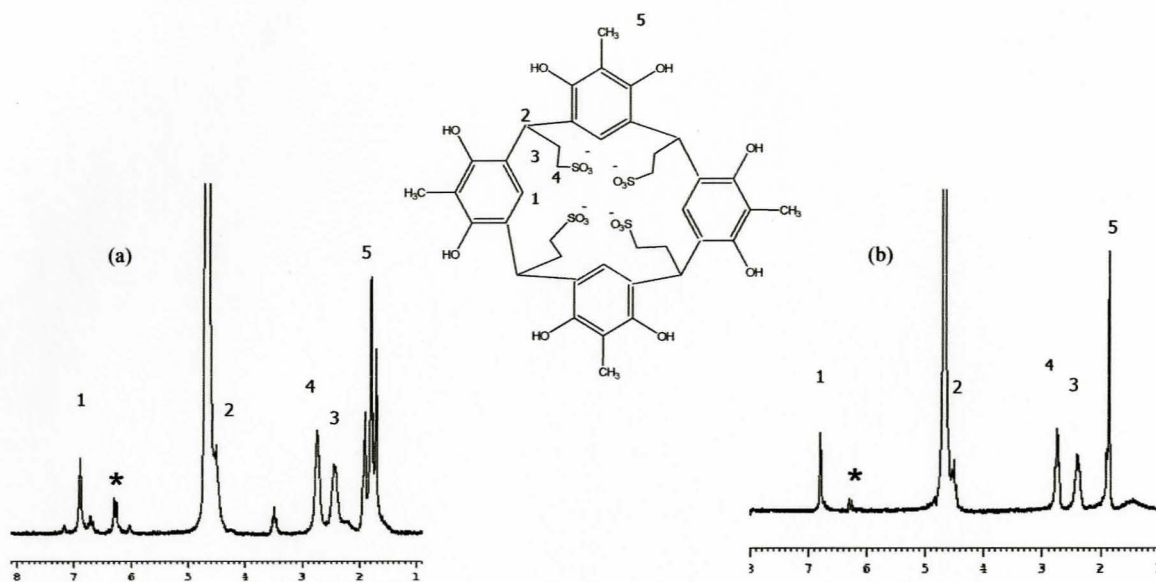


**Fig. 2.4**  $^1\text{H-NMR}$  spectra of (a) crude and (b) desalted TESMR that highlight five different proton resonances indicative of the *all-cis* configuration of the macrocycle.

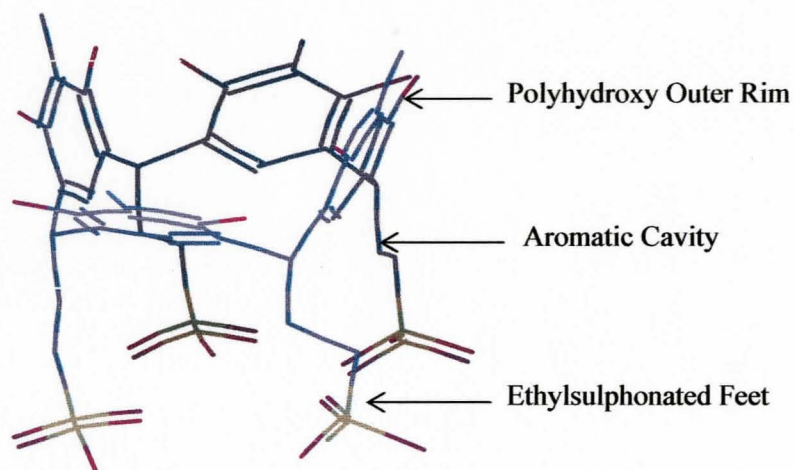


**Fig. 2.5** Energy-minimized 3D conformation of TESMR highlighting its major structural features

**Table 2.1** Different purification stages of TESMR as determined by  $^1\text{H-NMR}$

<i>TESMR Purification Stages</i>	<i>Relative Intensities</i>	
	<i>Peak 1 (ppm)</i>	<i>Peak* (ppm)</i>
Crude	100% (6.790)	50% (6.271)
1 <sup>st</sup> Recrystallization	100% (6.890)	40% (6.171)
2 <sup>nd</sup> Recrystallization	100% (6.816)	38% (6.212)
TFF desalting	100% (6.796)	3.5% (6.272)

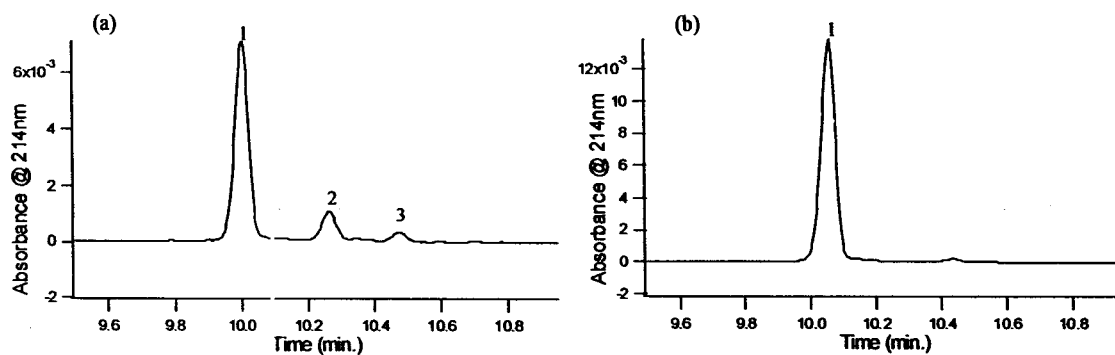


**Fig. 2.6** CE purity assay of (a) crude and (b) TFF-desalted TESMR

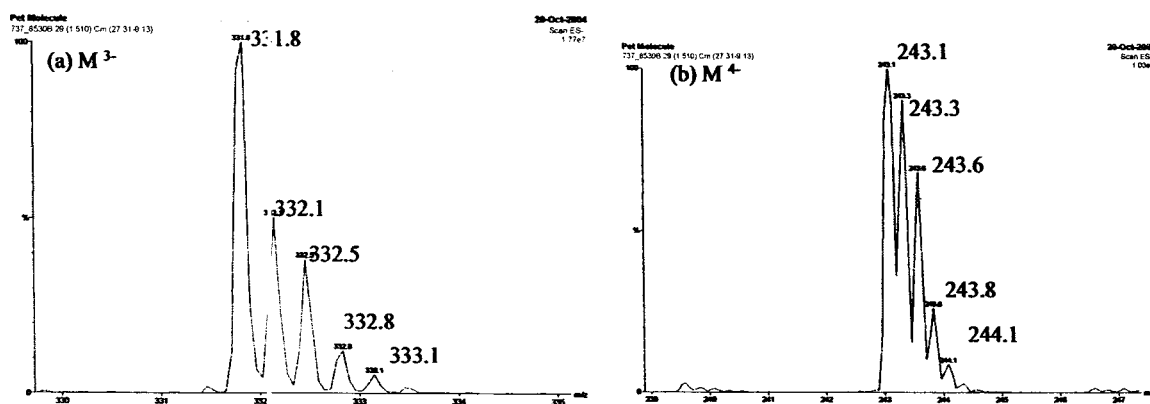


**Fig. 2.7** (a) Triply and (b) quadruply charged molecular anions of TESMR by ESI-MS.

ESI-MS was next used to confirm the molecular weight of TESMR. ESI was selected because it is a soft ionization method suitable for charged analytes that typically generate intact molecular ion envelopes that are reflective of its charged state. Since the presence of four sulphonic acid residues on TESMR impart a formal negative charge state, ESI was operated using a negative ion mode. The mass spectrum revealed both triply ( $M^{3-}$ ,  $m/z$  331.8) and quadruply ( $M^{4-}$ ,  $m/z$  243.1) charged species as shown in Fig. 2.7. Thus, the molecular weight of the compound was confirmed to be 972 Da, whereas its tetrasodium hydrated salt has a molecular weight of 1136 Da.

### 2.3.3 TESMR as an intrinsic buffer: $pK_a$ Determination by CE

The thermodynamic stability of the *all-cis* conformer of TESMR is primarily based on the formation of bridging H-bonds between adjacent phenolic hydroxyl moieties in the tetramer macrocycle. To date, the  $pK_a$  of resorcinarenes have not been fully examined. It can be expected that TESMR will be more acidic relative to its monomer precursor, 2-methyl resorcinol due to its unique macrocyclic structure. Knowledge of the  $pK_a$  values of TESMR is important for understanding its pH stability, electrophoretic mobility, spectroscopic and inherent buffer capacity properties. CE was used to measure the  $pK_a$  of three model compounds simultaneously, namely 2-methylresorcinol, *m*-nitrophenol and TESMR using phosphate and carbonate buffers ranging in pH from 6.0 to 11.0. Similar to the measuring of binding constants,  $pK_a$  values can be derived from CE experiments via the measurement of mobility changes as a function of buffer pH. The electrophoretic mobilities ( $cm^2/Vs$ ) were calculated using the following equation:

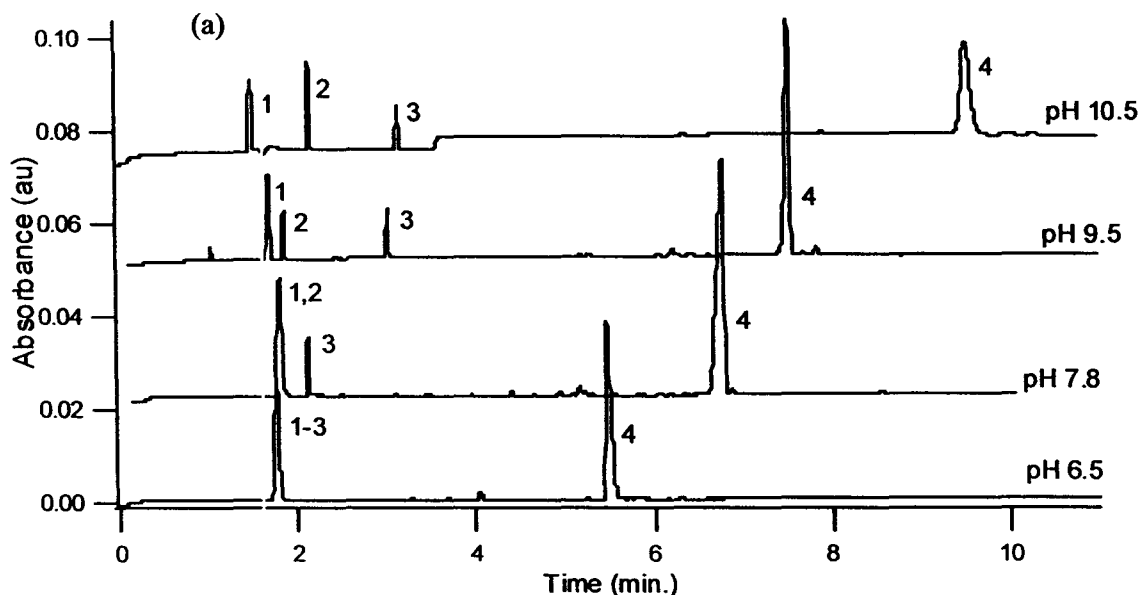


Fig.2.8 Electropherograms demonstrating specific changes in analyte mobility as a function of buffer pH for determination of  $pK_a$  by CE. 1-DMSO, 2-methyl resorcinol, 3-*m*-nitrophenol and 4-TESMR.

$$\mu_{ep} = \frac{L_c L_d}{V} \left( \frac{1}{t_{app}} - \frac{1}{t_{eof}} \right) \quad (1)$$

where  $L_c$  is the total capillary length,  $L_d$  is the effective capillary length (to detector),  $V$  is the applied voltage,  $t_{app}$  is the apparent migration time of a specific analyte and  $t_{eof}$  is the migration time of a neutral EOF marker.

As depicted in the overlay of electropherograms in Fig. 2.8, when performing CE experiments using a buffer pH of 6.5, *m*-nitrophenol and 2-methylresorcinol both are neutral and thus co-migrate with the EOF, whereas TESMR has a large negative mobility of  $-3.480 \times 10^{-4} \text{ cm}^2/\text{Vs}$ , which is reflected by a longer migration time. However, the mobility of *m*-nitrophenol slowly increases above  $\text{pH} > 7$  due to an increasing degree of ionization, whereas the mobility of 2-methylresorcinol does not change until  $\text{pH} > 9.5$  because of its relative weaker acidity.

The  $pK_a$  of a weak monoprotic (HA) and triprotic acid ( $H_3A^-$ ) can be determined by CE [13] via measurement of the analyte mobility shifts as a function of pH based on the following equations:

$$\mu_{ep}^{A^-} = \frac{K_a}{[H^+] + K_a} \mu_{ep,A^-} \quad (2)$$

$$\mu_{ep}^{A^-} = \frac{[H^+]^3}{d} \mu_{ep,H_3A^-} + \frac{[H^+]^2 K_{a1}}{d} \mu_{ep,H_2A^{2-}} + \frac{[H^+] K_{a1} K_{a2}}{d} \mu_{ep,HA^{2-}} + \frac{K_{a1} K_{a2} K_{a3}}{d} \mu_{ep,A^-} \quad (3)$$

where,  $d = [H^+]^3 + [H^+]^2 K_{a1} + [H^+] K_{a1} K_{a2} + K_{a1} K_{a2} K_{a3}$ . The ratio expression in front of each mobility term represents the fraction of analyte in a specific state. A plot of measured TESMR mobility as a function of buffer pH revealed three distinct mobility transitions (S-shaped titration curve) within the pH range studied suggestive of a weak triprotic acid system. In contrast, *m*-nitrophenol is a monoprotic weak acid and it undergoes a single and distinct mobility plot transition. As depicted in Fig. 2.9, the  $pK_a$  values of *m*-nitrophenol (used as a control) and TESMR were determined by iterative non-linear regression in which circles represent measured data (triplicates), solid lines are the predicted curve of best fit and dotted lines represent the upper and lower 95% confidence interval. The  $pK_a$  of *m*-nitrophenol (used as a control) was determined to be  $(8.29 \pm 0.05)$ , which is in close agreement with a literature value of 8.30 [14]. In contrast, the  $pK_a$  values of TESMR were estimated to be:  $pK_{a1} = (7.4 \pm 0.3)$ ,  $pK_{a2} = (9.1 \pm 0.3)$  and  $pK_{a3} = (9.9 \pm 0.3)$ . It is interesting to note about a 100-fold increase in acidity of TESMR relative to 2-methylresorcinol, which is reflected by the magnitude of  $pK_{a1}$  of 7.4 and 9.3, respectively. Since TESMR is a triprotic acid with closely spaced  $pK_a$  values, it can serve as a versatile intrinsic buffer in CE under neutral and alkaline conditions.

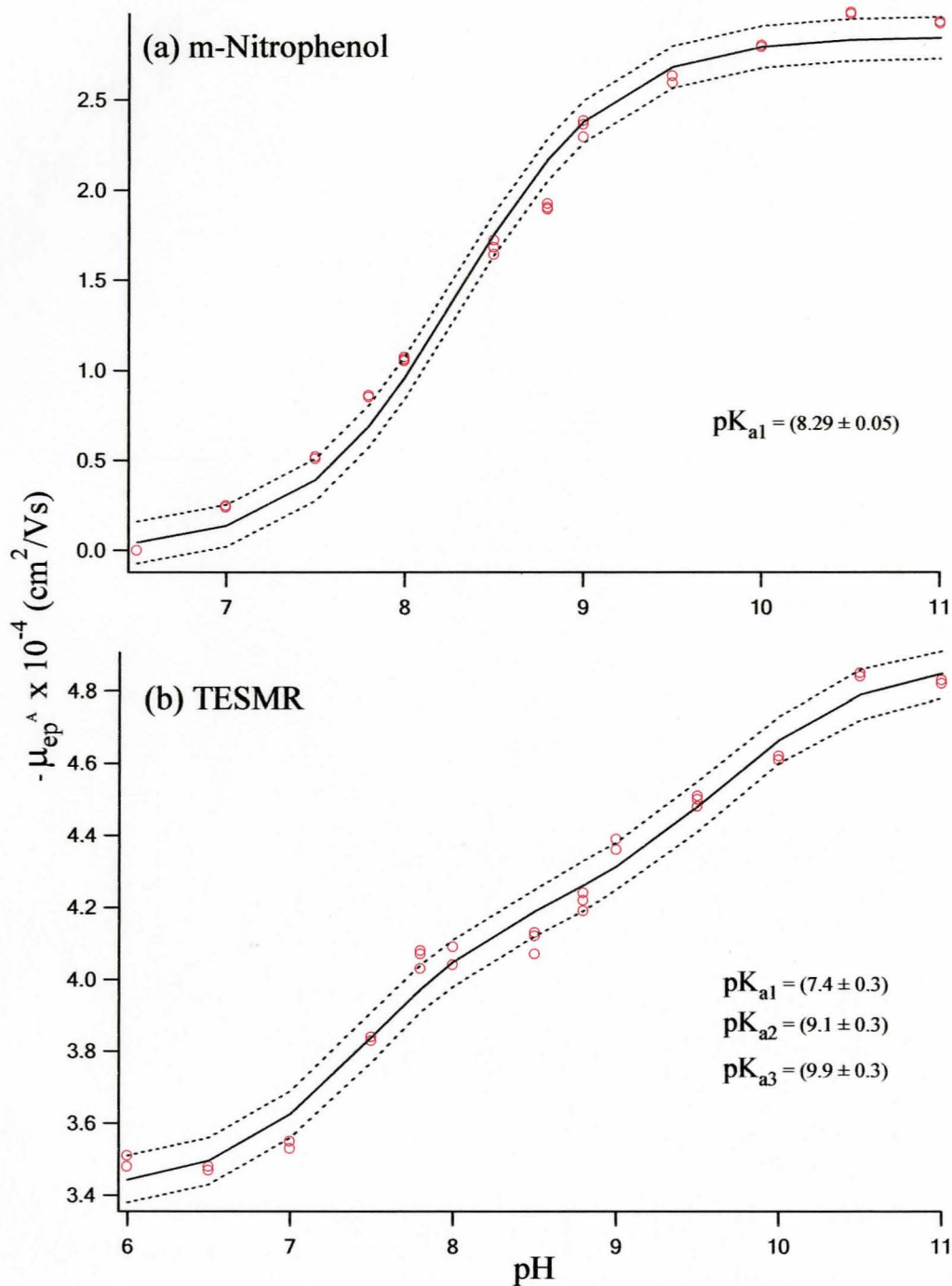


**Fig.2.9** Non-linear regression of mobility titration curves as determined by CE for the monoprotic acid (a) *m*-nitrophenol and the triprotic acid (b) TESMR

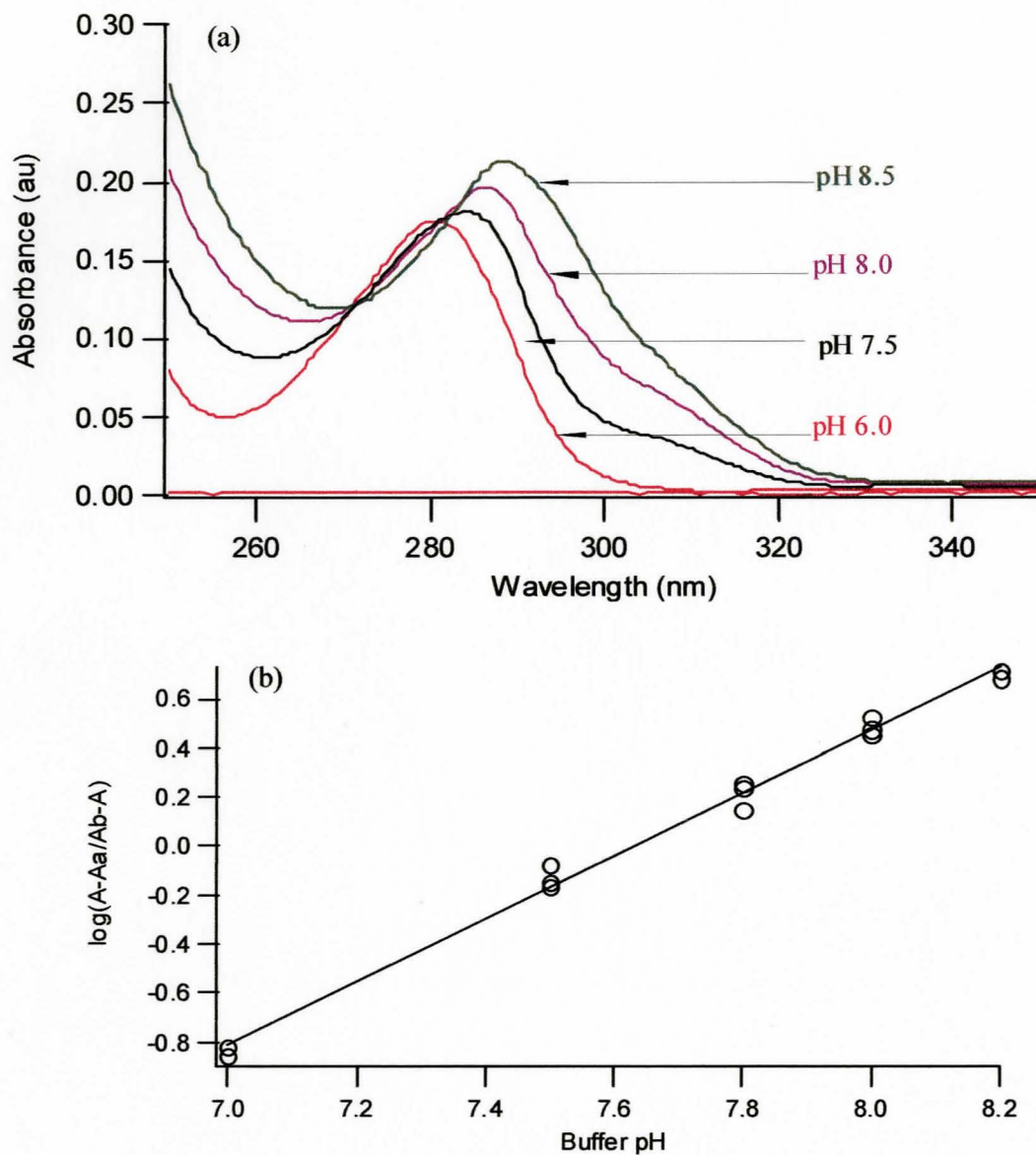


**Fig.2.10** (a) Overlay of UV absorbance spectra of 20  $\mu$ M TESMR as a function of buffer pH and (b) triplicate measurements of absorbance changes as a function of pH for  $pK_{a1}$  measurement.

### 2.3.4 TESMR spectroscopic properties

UV absorbance spectroscopy was also examined to estimate the  $pK_a$  of TESMR based on changes in absorbance as a function of buffer pH as depicted in **Fig. 2.10 (a)**. UV studies revealed that TESMR has two major absorbance bands centred at 202 nm and 280

nm at pH 6.0. It was observed that the 280 nm absorbance band underwent a significant bathochromic shift (red-shift) at pH > 6.5, as well as an increase in absorbance intensity when using 20  $\mu$ M TESMR in 50 mM phosphate buffer from pH 6.0 to 8.5. It was noticed that there were no further significant changes in absorbance properties at pH > 8.5. Based on previous CE experiments, the absorbance changes from pH 6.5 until pH 8.5 were ascribed to deprotonation of the first phenolic hydroxyl moiety of TESMR. The  $pK_{a1}$  of TESMR was then calculated using a modified version of the Henderson-Hasselbach equation described below:

$$pH = pK_a + \log \frac{(A - A_{HA})}{(A_{A^-} - A)} \quad (4)$$

where,  $A_{HA}$  and  $A_{A^-}$  represent the TESMR absorbance at pH 6.0 (fully protonated acid form) and pH 8.5 (fully deprotonated conjugate base form), respectively. Fig. 2.10 (b) also shows the linear plot based on triplicate measurements of absorbance changes as a function of pH using eq. 4. The  $pK_a$  value was estimated to be  $(7.6 \pm 0.5)$  which is in agreement with the  $pK_{a1}$  determined by CE.

To date, the fluorescence properties of resorcin[4]arenes have not been reported. The native fluorescence of TESMR was examined under various buffer conditions (buffer type, pH, solvent) as well as in polar aprotic solvents and compared relative to the natively fluorescent indoleamine tryptophan (Trp) which has a measured fluorescence quantum efficiency [15] of  $\Phi_F = 0.14$  in water. UV excitation at 266 nm was used since it closely matches the maximum absorbance of analytes and our laboratory is equipped with a solid-state UV laser with 266 nm emission, which can be used for CE analysis

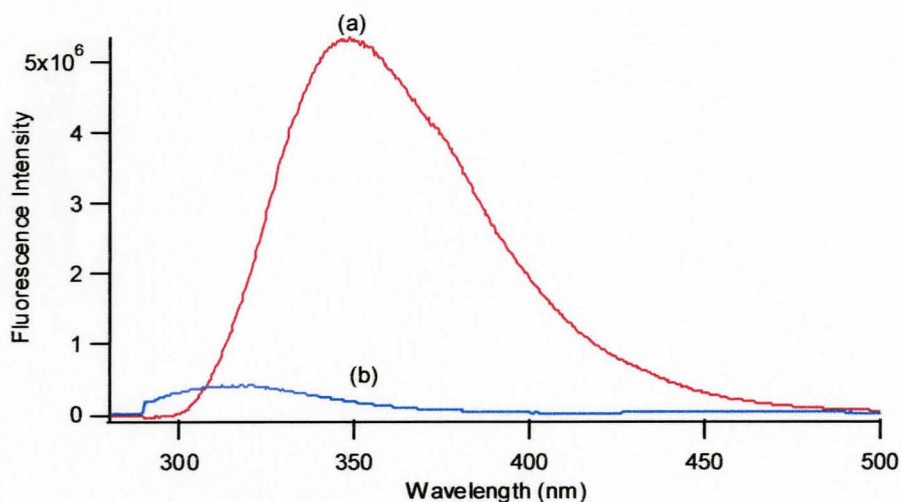


**Fig. 2.11** Fluorescence emission spectra of 2 $\mu$ M (a) TESMR and (b) Trp in dH<sub>2</sub>O using 266 nm excitation.

with on-capillary laser-induced native fluorescence (LINF) detection. **Fig. 2.11** compares the emission spectra of 2  $\mu$ M TESMR and Trp in de-ionized water. It was observed that TESMR possessed significant intrinsic fluorescence with an emission maximum centred at 316 nm. However, TESMR was about 12-fold less fluorescent than Trp reflected by a lower fluorescence quantum efficiency of approximately  $\Phi_F = 0.011$ . The less efficient fluorescence properties of TESMR relative to Trp can be explained in terms of the conformational flexibility of the macrocycle and the lack of a fused aromatic moiety similar to the indoleamine. It was determined that the fluorescence intensity and emission maxima of TESMR was influenced by buffer type, pH and solvent as summarized in **Table 2.2**; however, in all cases the fluorescence efficiency was enhanced in de-ionized water with a relative order of dH<sub>2</sub>O > acidic buffer > polar aprotic solvent > basic buffer. The native fluorescence properties of TESMR may be used as a mechanism for detection of bound non-fluorescent analytes via fluorescence enhancement or

**Table 2.2** Influence of solution properties on intrinsic fluorescence of TESMR

<i>TESMR/Solution</i>	<i>Intensities</i>	<i><math>\lambda_{em}</math> (nm)</i>
dH <sub>2</sub> O	$(4.44 \pm 0.48) \times 10^5$	316
Phosphate pH 1.8	$(3.22 \pm 0.14) \times 10^5$	323
Borate pH 9.5	$(3.30 \pm 0.07) \times 10^4$	303
DMSO	$(1.70 \pm 0.16) \times 10^5$	305
Tryptophan in dH <sub>2</sub> O	$(5.65 \pm 0.14) \times 10^6$	347

quenching during electromigration in CE, which can provide lower detection limits for sub-micromolar detection of analytes without chemical derivatization. Further enhancement of TESMR intrinsic fluorescence properties can potentially be improved by synthesizing more conformationally-rigid methylene-bridged cavitand derivatives [16] that undergo less probable non-radiative relaxation pathways.

### 2.3.5 TESMR buffer capacity

Our long-term research goal is to develop a resorcinarene-based additives for single-step CE analyses of steroid metabolites, which can be used to enhance molecular recognition by combining thermodynamic properties and conformational selectivity via dynamic inclusion complexation during electromigration. Given the weakly acidic polyprotic properties of TESMR, it can also serve as an intrinsic buffer without interferences from buffer electrolyte co-ions which may alter analyte binding affinity or change spectroscopic properties. The buffer in CE plays an essential role as mobile ion carriers to complete the electrical circuit under the applied voltage across the capillary, as well as resist pH changes due to the electrolysis of water at the platinum electrodes during separation. Buffer pH also plays a vital role in the selectivity of separation of weakly ionic analytes by controlling the degree of ionization and thus its electrophoretic

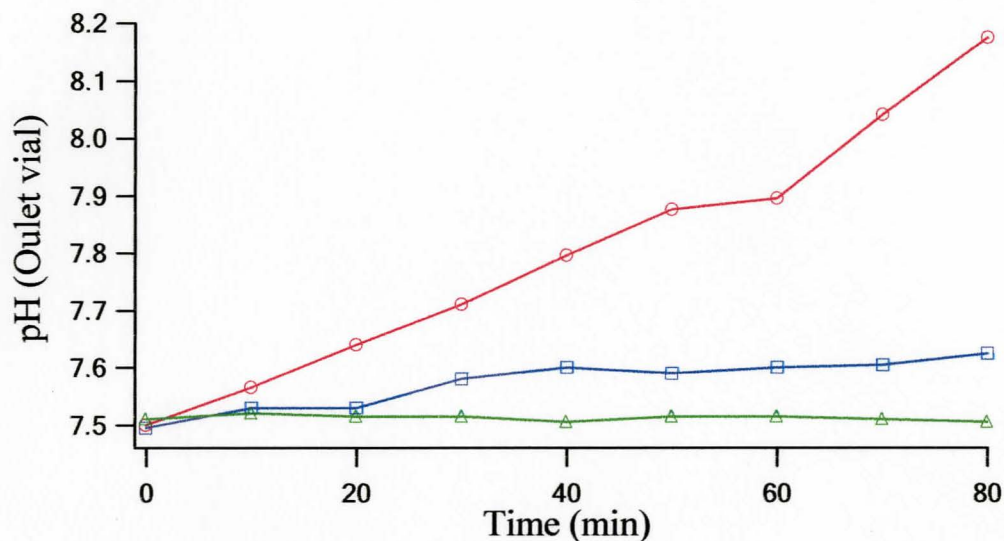


**Fig. 2.12** Buffer capacity assessment by CE of 20 mM TESMR, pH 7.5 ( $\Delta$ ), relative to phosphate buffer (buffer control,  $\square$ ) and dichromate (non-buffer control,  $\circ$ ).

mobility. The inherent buffer capacity is related to the relative difference of solution pH to  $pK_a$  and total ionic strength which controls the relative concentrations of weak acid and conjugate base. The buffer capacity of three different electrolyte co-anions (TESMR, phosphate and chromate) with a concentration of 20 mM and adjusted to a pH of 7.5 with NaOH was examined by CE by measuring the pH and current changes over time in the buffer inlet and outlet reservoirs during electrophoresis under a voltage of +20 kV. The pH changes of TESMR ( $pK_{a1} = 7.4$ ) was compared relative to a well-characterized buffer, namely phosphate ( $pK_{a2} = 7.2$ ) and a non-buffered electrolyte (control) chromate, which is a common anionic probe used for indirect UV detection in CE [17, 18]. Changes in solution pH and current (conductivity) can be expected over time due to the increasing production of conductive  $H^+$  and  $OH^-$  ions caused by water electrolysis in the buffer inlet and outlet reservoirs, respectively. **Fig. 2.12** depicts an overlay plot comparing the

measured pH and current changes of the buffer outlet as a function of time. It is apparent that chromate solution undergoes rapid increases in pH and current because it is a strong acid that is unbuffered. In contrast, TESMR was observed to maintain a constant pH and current profile throughout the time range which was examined to a greater extent than phosphate. Thus, TESMR can be used as a stable electrolyte ion carrier in CE with a high buffering capacity without the requirement of additional buffer salts in solution.

## 2.4 Conclusion

TESMR was synthesized, purified and fully characterized using several different techniques, including  $^1\text{H-NMR}$ , CE, ESI-MS, UV absorbance and fluorescence spectroscopy. Desalting by TFF was important to future CE binding studies in order to minimize Joule heating caused by the excess mobile salts in the product, as well as reduce electrolyte interferences that can modify apparent binding constant measurements. CE was used as a versatile technique to characterize TESMR purity, measure its  $\text{pK}_a$  values, as well as assess its buffer capacity and ion transport properties. To the best of our knowledge, this work represents the first example of a macrocycle which can be used as both an intrinsic buffer and electrokinetic host for enhanced inclusion complexation of small guests by CE. Further work will investigate ways to improve the intrinsic fluorescence properties of resorcin[4]arene derivatives.

## 2.5 References

- [1] Asfari, Z.; Bohmer, V.; Harrowfield, J.; Vicens, J., "Calixarenes 2001"; Kluwer Academic Publishers, The Netherlands, 2001.
- [2] Rekharsky, M. V.; Inoue, Y., *Chem. Rev.* **1998**, *98*, 1875-1917.
- [3] Diederich, F., "Cyclophanes", Royal Society of Chemistry, Ed.: J. F. Stoddart, Cambridge, 1991.
- [4] Ma, J. C.; Dougherty, D. A., *Chem. Rev.* **1997**, *97*, 1303-1324.
- [5] Hunter, C. A., *Chem. Soc. Rev.* **1994**, 101-109.
- [6] Nishio, M.; Hirota, M.; Umezawa, Y., *Tetrahedron* **1995**, *51*, 8665-8701.
- [7] Arduini, A.; Pochini, A.; Reverberi, S.; Ungaro, R., *J. Chem. Soc. Chem. Commun.* **1984**, 981-982.
- [8] Bachmann, K.; Bazzanella, A.; Haag, I.; Han, K., *Anal. Chem.* **1995**, *67*, 1722-1726.
- [9] Kazakova, E. K.; Ziganshina, A. U.; Muslinkina, L. A.; Morozova, J. E.; Makarova, N. A.; Mustafina, A. R.; Habicher, W. D., *J. Incl. Phenomena Macrocyclic Chem.* **2002**, *43*, 65-69.
- [10] Kunsza, S.; Szabo, K. L.; Lemli, B.; Bitter, I.; Nagy, G.; Kolla, L., *J. Phy. Chem. B* **2004**, *108*, 15519-15522.
- [11] Kobayashi, K.; Asakawa, Y.; Kato, Y.; Aoyama, Y., *J. Am. Chem. Soc.* **1992**, *114*, 10307-10313
- [12] Britz-McKibbin, P.; Chen, D. D. Y., *Anal. Chem.* **1998**, *70*, 907-912.
- [13] Bohmer, V., *Angew. Chem. Int. Ed. Engl. (Review)* **1995**, *34*, 713-745.
- [14] Poole, S. K.; Patel, S.; Dehring, K.; Workman, H.; Poole, C. F., *J. Chromatogr. A*

2004, 1037, 445-454.

[15] Suh, J.; Koh, D.; Min, C., *J. Org. Chem.* **1988**, 53, 1147-1153.

[16] Eaton, D., *Pure Appl. Chem.* **1988**, 60, 1107-1114.

[17] Roman, E.; Peinador, C.; Mendoza, S.; Kaifer, A. E., *J. Org. Chem.* **1999**, 64, 2577-2578.

[18] Marion, K.; Brett, P.; Haddad, P. R.; Miroslav, M., *Analyst* **2002**, 127, 1564-1567.

[19] Breadmore, M. C.; Haddah, P. R.; Fritz, J. S., *J. Chromatogr. A* **2002**, 920, 31-40.

## CHAPTER 3

### Enhanced Binding and Conformational Selectivity in Affinity Capillary Electrophoresis using a Water-soluble Resorcin[4]arene

#### Abstract

Affinity capillary electrophoresis (ACE) is a widely used technique for quantifying non-covalent molecular interactions that is dependent on the specific buffer conditions selected. In this study, dynamic 1:1 host-guest inclusion complexation involving a charged resorcin[4]arene with a group of neutral corticosteroids was examined by ACE, where the macrocycle serves as both an intrinsic buffer and electrokinetic host. It was determined that over a 200 % enhancement in the apparent binding constant ( $K_B$ ) was realized by ACE when using the host as an intrinsic buffer at pH 7.5 relative to an extrinsic sodium phosphate buffer system, which was also confirmed by  $^1\text{H-NMR}$  experiments. This report also revealed improved selectivity (up to 30 %) mediated by the discrete conformational properties of the complex among similar corticosteroid guests, as reflected by the complex mobility ( $\mu_{ep, AC}$ ) or the relative change in complexation-induced mobility ( $1 - \mu_{ep, AC} / \mu_{ep, C}$ ). This latter property is a unique feature of ACE reflective of hydrodynamic size selectivity involving bulky guests or substrates, which is often unexplored in conventional measurements.  $^1\text{H-NMR}$  and computer molecular modeling provided complementary information regarding the relative orientation, conformation and overall molecular area of the complex. The coupling of thermodynamic ( $K_B$ ) and electrokinetic ( $\mu_{ep, AC}$ ) factors related to complex formation in

buffered solutions that minimize the effects of extrinsic electrolytes serves to enhance enthalpy-driven molecular recognition processes by ACE.

### 3.1 Introduction

Affinity capillary electrophoresis (ACE) is a versatile technique for assessing non-covalent molecular interactions in free solution provided that there are significant changes in apparent substrate mobility as a result of specific complexation [1-4]. Depending on the magnitude of binding affinity, kinetics of interaction and sensitivity required, ACE can be performed using several different formats, such as non-equilibrium [5], frontal analysis [6], vacancy [7] and partial filling [8] methods. For weak to moderate interactions ( $K_B < 10^3 \text{ M}^{-1}$ ) involving host-guest inclusion complexation (*e.g.*, cyclodextrin), ACE is most conveniently performed via dynamic complexation of multiple guests simultaneously during electromigration based on measured mobility shifts. Extremely weak interactions can be measured accurately when an appropriate concentration range of host is used in the run buffer to assess the binding isotherm (fraction of complex,  $f_{AC}$  0.2-0.8) and suitable correction factors are applied to normalize changes in analyte mobility not associated with specific binding, such as bulk solution viscosity and dielectric constant [9, 10]. A common feature to all ACE formats is the composition of the buffer (*e.g.*, buffer type, pH, ionic strength), which plays a crucial role in optimizing the mobility of weakly ionic guests relative to host in order to ensure maximum mobility shifts upon complexation, as well as providing stable pH and ion transport properties during electrophoresis required for precise mobility measurements.

Moreover, the buffer composition has a direct impact on the apparent binding constant ( $K_B$ ) derived from ACE experiments by modifying the extent of electrostatic shielding, dipole interactions and solute hydration, which can significantly alter the affinity of host-guest complexation. Improved understanding of the impact of buffer composition in non-covalent molecular interactions is important for enhancing selectivity in ACE, as well as developing accurate models for  $K_B$  prediction based on computer simulations [11, 12].

One of the unique features of ACE is that both thermodynamic (equilibria) and electrokinetic (mobility) parameters associated with complex formation can be used for improved selectivity in molecular recognition. To date, the majority of ACE applications have been primarily directed at measuring thermodynamic and rate constants as a rapid and alternative format relative to conventional techniques based on optical spectroscopy, NMR, equilibrium dialysis and chromatography. However, in the case of molecular interactions involving bulky guests or high molecular weight substrates (*e.g.*, protein-protein interactions), the specific conformation, hydrodynamic size and shape of the complex can represent an important parameter influencing selectivity in ACE experiments, as reflected by the complex mobility,  $\mu_{ep, AC}$ . In most cases, conformational selectivity in ACE, such as protein folding is considered only in terms of its influence on binding affinity [13] rather than the conformation of the complex as a whole. Vigh *et al.* [12] previously reported that size selectivity in chiral ACE as characterized by the ratio of complex mobilities of each enantiomer can provide a significant contribution to overall selectivity in addition to binding affinity. Further work is needed to better understand the impact of complex mobilities in ACE, which can provide insight regarding the unique

conformational properties of the complex in solution.

Resorcin[4]arenes [14] belong to an important class of synthetic receptor that are widely used as models for understanding non-covalent interactions. They also serve as useful precursors for constructing conformationally-rigid cavitands [15], and non-covalent resorcinarene capsule assemblies [16]. There have been several reports of using charged resorcin[4]arenes as novel additives for separation of neutral analytes by CE [17-20], however quantitative understanding of their interaction by ACE has yet to be explored. In this study, the *C*-tetraethylsulphonate derivative of 2-methyl resorcinarene (TESMR) was used as the host because of its high aqueous solubility, large negative mobility and flexible structure for accommodating a variety of guests [19, 21]. The non-covalent interactions between TESMR and a group of neutral corticosteroid metabolites that differ by a single functional group were selected as a model charged host-neutral guest system. To the best of our knowledge, this report introduces three new concepts relevant to fundamental ACE studies, namely: 1) a weakly ionic host or receptor can serve as an intrinsic buffer and electrokinetic host without extrinsic electrolytes providing up to a 200 % enhancement in apparent affinity, 2) up to 30 % of the overall selectivity in ACE can be influenced by differences in the hydrodynamic size associated with inclusion complex formation, and 3) computer molecular modeling together with NMR studies can provide complementary information to ACE data regarding binding affinity and complex conformation. The polyprotic weak acidity and buffer capacity of TESMR

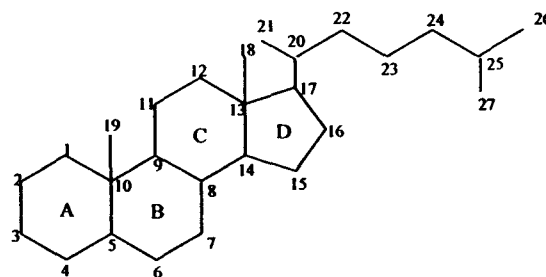


**Fig.3.1** Cyclopentaphenanthrene ring skeleton and numbering of steroid ring structure

was examined by CE, which revealed that the host can serve as intrinsic buffer at pH 7.5 with extremely stable current and pH profiles relative to phosphate buffer during electrophoresis. Noteworthy, this study demonstrated a direct correlation between measured  $K_B$  and  $\mu_{ep, AC}$  parameters, indicating that higher affinity was associated with more compact inclusion complexes with a reduced average hydrodynamic size, as reflected by the magnitude of the relative change in complexation-induced mobility ( $1 - \mu_{ep, AC} / \mu_{ep, C}$ ). Insight into the specific conformational properties of the complex when using TESMR as an intrinsic buffer and electrokinetic host in ACE were also compared using  $^1\text{H-NMR}$  and computer molecular modeling.

### 3.2 Corticosteroids

Steroids represent a diverse sub-class of neutral hydrophobic biomolecules that play important roles as chemical modulators and hormones possessing a common cyclopentaphenanthrene framework, as shown in Fig. 3.1. The test guest steroids in this study used for examining TESMR inclusion complexation are a group of corticosteroids or glucocorticoids, which are characterized by an oxygen functionality (*e.g.*, alcohol,

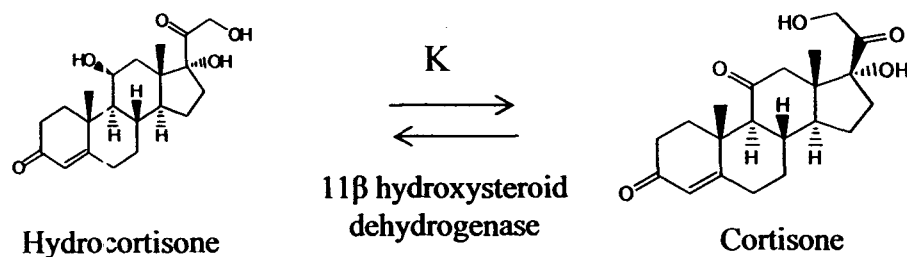
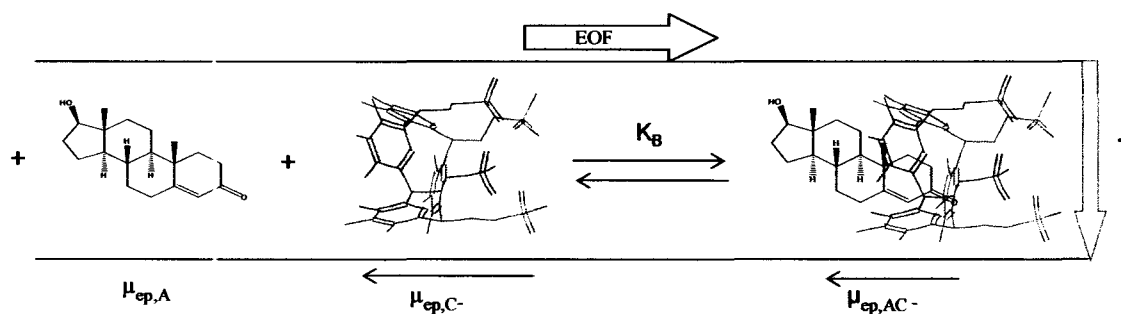


**Fig.3.2** Enzymatic conversion of hydrocortisone to cortisone

ketone) at C<sub>11</sub>. These steroids are biologically relevant hormones involved in a wide range of physiological systems such as stress and immune response, regulation of glucose metabolism and inflammation [22]. For example, the enzyme 11β-hydroxysteroid dehydrogenase (11β-HSD) catalyses the interconversion of hydrocortisone (biologically-active) to cortisone in the body, as depicted in Fig. 3.2. It has been reported that the renal isoenzyme of 11β-HSD has a lower affinity for the product cortisone, thus favoring the conversion of hydrocortisone to cortisone, thereby protecting the kidneys from excessive hydrocortisone activity [23]. In this study, enhanced molecular recognition of neutral bulky corticosteroids that differ by a single functional group will be demonstrated with the synthetic macrocycle TESMR based on differential affinity and conformational selectivity in ACE.

### 3.3. Theory

Selective analysis of steroid mixtures by CE is challenging since they are electrically neutral with a wide range of isomeric structures. MEKC is the most widely used approach for steroid analysis [24] via differential partitioning within mobile charged



**Scheme 3.1:** A pictorial illustration of 1:1 dynamic inclusion complexation during electromigration in ACE micelles (*e.g.*, SDS) that are included in the run buffer. In this study, TESMR is used as a discrete resorcin[4]arene macrocycle for differential inclusion complexation of corticosteroids. Since the chemical structures of resorcin[4]arenes are more well defined than micellar supramolecular assemblies, deeper insight into the mechanism of complexation can be derived. Moreover, since the average molecular area of TESMR relative to corticosteroids are more similar in magnitude, subtle differences in steric and conformational properties of the complex can be more readily distinguished. To the best of our knowledge, this is the first report that examines resorcin[4]arene-steroid interactions in aqueous solution by ACE. Based on dynamic 1:1 inclusion complexation during electromigration in ACE, changes in the viscosity-corrected apparent mobility ( $v\mu_{ep}^A$ ) of neutral corticosteroids as a function of TESMR concentration can be described by **Scheme 3.1** and eq. (1):

$$v\mu_{ep}^A = \frac{K_B [C]}{1 + K_B [C]} \mu_{ep,AC} \quad (1)$$

where,  $K_B$  is the apparent binding constant,  $[C]$  is the concentration of TESMR and  $\mu_{ep,AC}$  is the complex mobility. Thus, the separation of neutral corticosteroids using

TESMR in ACE is based on differences in  $K_B$  and  $\mu_{ep, AC}$ . In cases where two steroids have similar binding affinity, differences in the hydrodynamic size, shape and conformation of the complex, as reflected by  $\mu_{ep, AC}$  can be used as a basis for molecular recognition. At a given concentration of TESMR, neutral analytes with a higher affinity will have the greatest increase in apparent negative mobility reflected by longer migration times. In fact, ACE can be used as a tool to measure the apparent binding constants of multiple analytes [25] from impure samples using nanoliters of volume based on the measurement of mobility shifts as a function of additive concentration. Note that when performing dynamic complexation studies under high electric fields in unmodified fused-silica capillaries, the EOF is typically directed towards the cathode under normal polarity setting.

### 3.4 Experimental

#### 3.4.1 Chemicals and Reagents

De-ionized water for buffer and sample preparations was obtained using a Barnstead EASYpure®II LF ultrapure water system (Dubuque, Iowa, USA). 2-(2-bromoethyl)-1,3-dioxane, 2-methylresorcinol, deuterium oxide ( $D_2O$ ), *m*-nitrophenol, hydrocortisone (HC), cortisone (C) and corticosterone (CC) were purchased from Sigma-Aldrich Inc. (St. Louis, USA). The background electrolyte buffers for TESMR  $pK_a$  and corticosteroid binding studies were prepared using dihydrogen sodium phosphate, sodium bicarbonate and sodium tetraborate decahydrate. HPLC grade methanol was purchased from Caledon Laboratories Ltd. (Georgetown, Canada). Dihydrogen sodium phosphate, sodium

tetraborate decahydrate and sodium bicarbonate were obtained from Sigma-Aldrich. The buffer pH was modified by using 0.1 M NaOH to obtain the desired pH.

### **3.4.2 TESMR synthesis and purification**

The synthesis of TESMR was performed according to the procedure by Aoyama *et al.* [21] and the all-cis conformer was purified by repeated recrystallization in 1:1 MeOH:H<sub>2</sub>O and then desalted by tangential flow fractionation using a Minimate<sup>TM</sup> cartridge with 1000 Da MWCO filter (Pall Corporation, Mississauga, ON). The desalting of TESMR was monitored by measuring the retentate conductivity using a MC 126 (Mettler Toledo, Mississauga, ON) conductivity meter over three hours until no further significant conductivity changes were noted. This was deemed important since excess electrolytes can alter the apparent binding constant, as well as contribute to Joule heating and higher currents during CE experiments. The purity of TESMR was confirmed to be approximately 96 % by <sup>1</sup>H-NMR and CE.

### **3.4.3 Capillary electrophoresis**

All separations were performed on an automated P/ACE 2100 CE system (Beckman-Coulter Inc., Fullerton, CA, USA). Uncoated fused-silica capillaries with 50 µm i.d., 360 µm o.d. and 67 cm length (Polymicro Technologies, Phoenix, AZ, USA) were used for analyses. Separations began by rinsing the capillary for 5 min with 0.1 M NaOH, followed by a 5 min rinse with buffer. Separations were performed thermostated at 25 °C using 25 kV and UV absorbance was monitored at 254 nm. Hydrodynamic injection of

sample was performed on to the capillary inlet using a low pressure (0.5 psi or 3.5 kPa) for 3 s.  $pK_a$  measurements by CE were performed using a buffer pH range from 6 to 11.0 (20 mM phosphate or carbonate) using a 40  $\mu$ M sample mixture consisting of TESMR, 2-methylresorcinol (monomer precursor) and *m*-nitrophenol (control). TESMR binding experiments by ACE were performed using 20 mM phosphate, pH 7.5 as an extrinsic buffer or TESMR as an intrinsic buffer (without phosphate) at pH 7.5 in 0.5 % methanol with 60  $\mu$ M of the three model corticosteroids as the sample. Under most conditions, the fraction of complex was examined from about 20 % to 70 % in order to reduce error associated with  $K_B$  and  $\mu_{ep, AC}$  values from binding isotherms. 1:1 binding stoichiometry was confirmed by linear transformation of binding isotherms into x-reciprocal plots, which are sensitive to higher order interactions [26]. The complexation-induced changes in apparent mobility of corticosteroids were measured using nine different TESMR solutions ranging from 0-10 mM. Non-linear regression was performed using Igor Pro 4.0 (Wavemetrics Inc., Lake Oswego, USA) to obtain  $K_B$  and  $\mu_{ep, AC}$  parameters by CE with  $\chi^2$  as a measure of deviation between data points and fitted curve. The relative viscosity correction factor ( $\nu$ ) needed to normalize corticosteroid apparent mobilities was measured using CE by comparing the average time ( $n = 5$ ) for a sample plug to travel to the detector window using a low pressure rinse (0.5 psi) at a specific concentration of TESMR (0.5-10 mM) relative to 0 mM TESMR. It was determined that significant changes in solution viscosity occurred at concentrations  $> 3$  mM with a maximum viscosity increase of about 4.2 % at 10 mM TESMR. Buffer capacity experiments were performed by CE using an electric field strength of 425  $Vcm^{-1}$

for all solutions over 80 min, during which the voltage was temporarily halted and the pH at the outlet buffer reservoir (cathode) was measured at a 10 min interval.

### 3.4.4 $^1\text{H-NMR}$

$^1\text{H-NMR}$  spectra were recorded on a Bruker AV200 spectrometer for TESMR purity and characterization studies using  $\text{D}_2\text{O}$  as the solvent. Five proton resonances were observed for TESMR, namely  $\text{CH}$  6.796 ppm,  $\text{CH}$  4.505 ppm,  $\text{CH}_2$  2.726 ppm,  $\text{CH}_2$  2.382 ppm and  $\text{CH}_3$  1.852 ppm, similar to a previous report.<sup>19</sup> Singlet aromatic and methyl proton resonances were consistent with the symmetrical bowl-shaped conformation of the tetramer. TESMR-HC binding experiments by  $^1\text{H-NMR}$  were performed using a Bruker AV 600 spectrometer with  $\text{D}_2\text{O}$  and 0.5 %  $\text{CD}_3\text{OD}$  as the solvent using 128 scans with solvent suppression. The concentration of HC was fixed at 0.2 mM, whereas TESMR was varied using six solutions ranging from 0-8 mM. The complexation-induced changes in chemical shift of three proton resonances for HC were used to obtain  $K_B$  and  $\Delta_{\text{max}}$  or  $(\delta_{\text{AC}} - \delta_{\text{A}})$  by non-linear regression [27]. The three resolved HC proton resonance peaks that were not overlapped by TESMR or solvent signals corresponded to H4 ( $\text{CH}$ , 5.693 ppm), H18 ( $\text{CH}_3$ , 1.316 ppm) and H19 ( $\text{CH}_3$ , 0.760 ppm). All proton resonances were observed to undergo lower frequency induced chemical shifts upon complexation with TESMR. Van't Hoff plots were used to derive  $\Delta\text{H}^\circ$  and  $\Delta\text{S}^\circ$  parameters using HC-TESMR (intrinsic buffer, pH 7.5) over the same concentration range as previous experiments over five different temperatures ranging from 283-303 K using the H18 resonance frequency of HC. The temperature of the probe

was verified to be within  $\pm 0.1$  K using a thermocouple device. The temperature range was kept small in order to minimize deviations related to temperature-independence of enthalpy and entropy.

### **3.4.5 Computer molecular modeling**

Qualitative insight into a stable conformation and orientation of the TESMR-HC complex was performed by CHEM 3D Ultra 8.0 (CambridgeSoft, Cambridge, USA). Molecular mechanics (MM2) force field was first used for energy minimization of isolated TESMR and HC structures based on steric and non-covalent interactions. TESMR and HC structures were docked together and an iterative MM2 energy minimization and molecular dynamics sequence of experiments were performed until a global minimum in the energy of the complex was reached. The interaction energy ( $\Delta E$ ) of inclusion complexation was favourable and it was estimated to be about  $-16.0$  kcal mol<sup>-1</sup> by comparing the energy of isolated structures to most stable complex conformation. The molecular area (Connelly) of the HC-TESMR complex relative to free TESMR was also calculated to estimate the relative increase in molecular radius. It should be noted that computer modeling neglects solvent contributions to interaction and it was mainly used to provide qualitative information regarding a stable TESMR-HC complex conformation in relation to CE and NMR data.

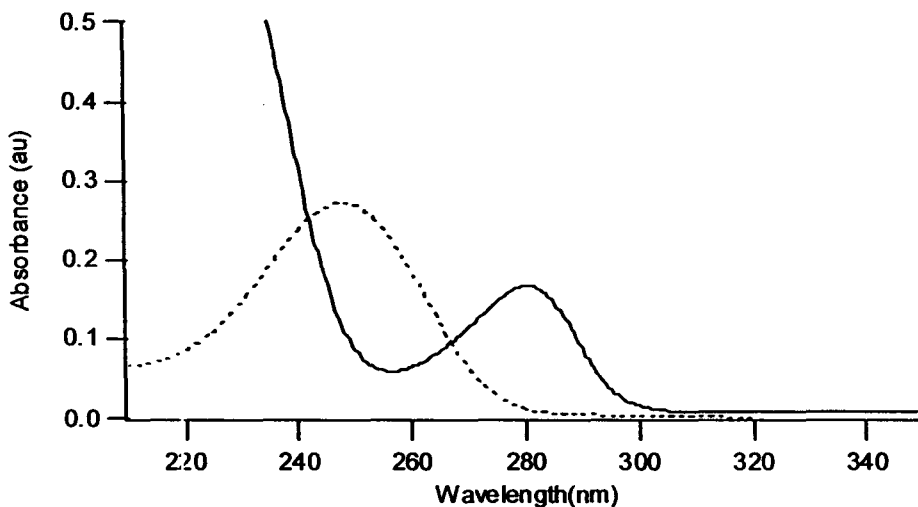


Fig. 3.3 Overlay UV absorbance spectra of TESMR (solid line) and HC (dotted line).

### 3.5 Results and Discussion

#### 3.5.1 TESMR and steroid spectroscopic properties

The UV spectral properties of corticosteroids and TESMR were compared as illustrated in Fig. 3.3. Note that the major absorption band for hydrocortisone (*e.g.*, enone) was at 248 nm, which occurs in a spectral window where TESMR has weak absorbance. This is significant since it permits the direct detection of corticosteroids in the presence of high concentrations of TESMR by CE with UV detection using a 254 nm bandpass filter. The molar absorptivity of HC was about  $1.2 \times 10^4 \text{ L}^{-1}\text{cm}^{-1}$ , which was over 4-fold greater than TESMR at 254 nm.

#### 3.5.2 TESMR as intrinsic buffer and electrokinetic host in ACE

There have been only two previous reports [28, 29] of the binding of resorcin[4]arenes with bulky steroids, which were performed by  $^1\text{H-NMR}$  in  $\text{CDCl}_3$  due

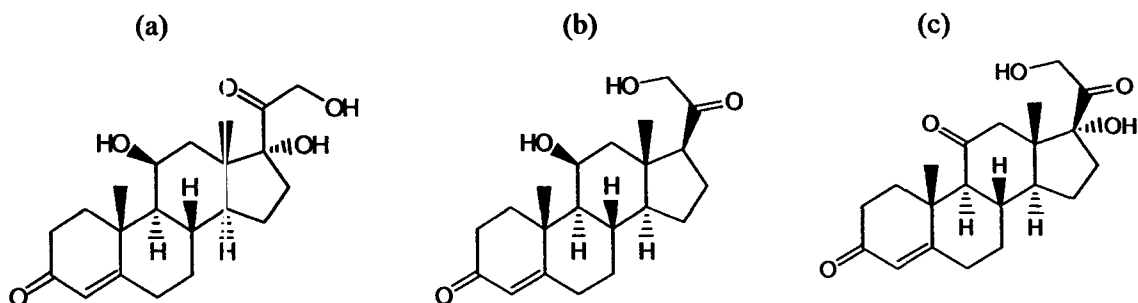
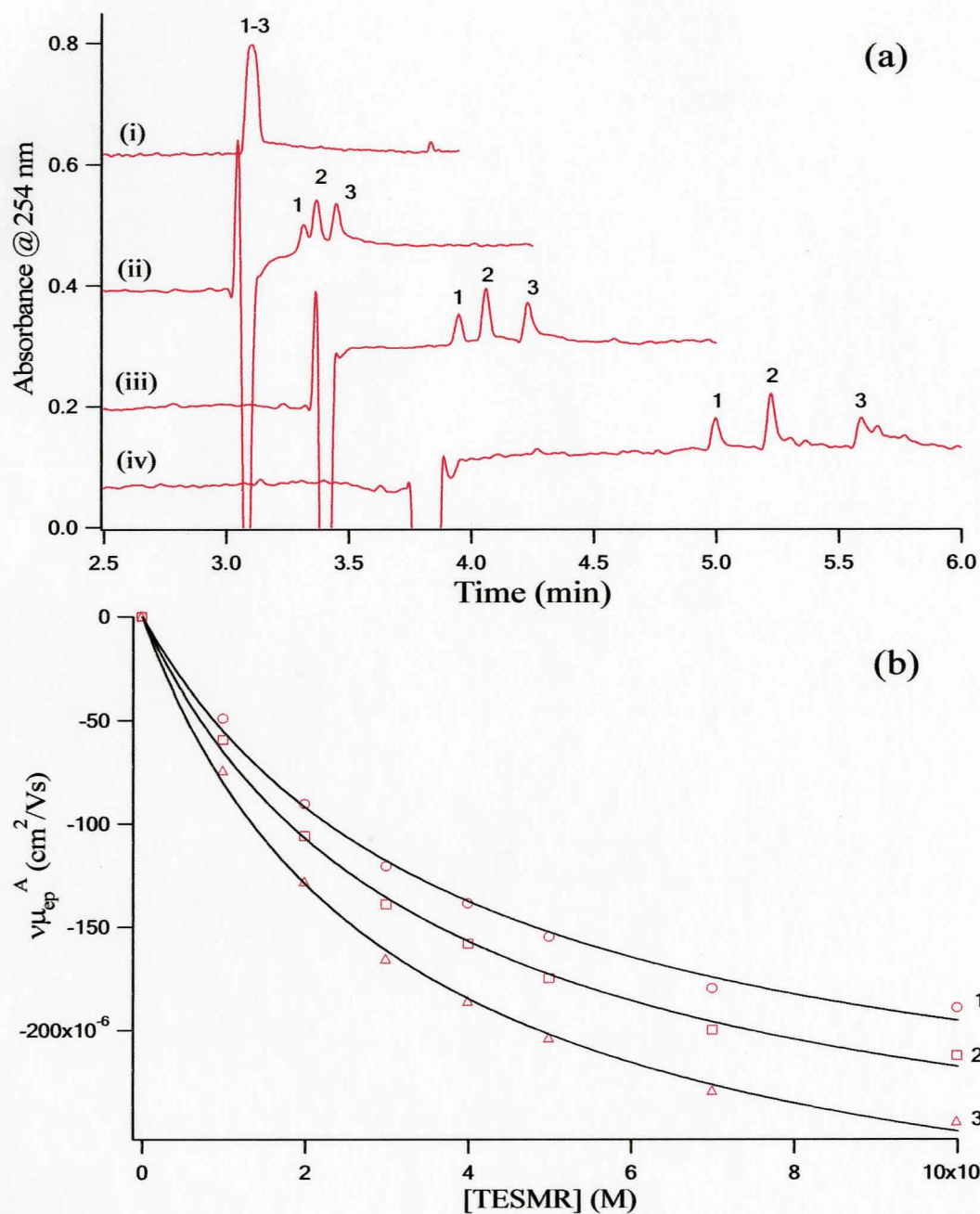


Fig. 3.4 Chemical structures of the model corticosteroid guests (a) HC, (b) C and (c) CC

to the limited aqueous solubility constraints dictated by either host or guest. Although weak steroid binding had been observed in these studies, improved selectivity in aqueous systems can be realized when examining the unique binding and conformational properties of the host-guest complex by ACE without extrinsic electrolytes. The focus of this study was to quantitatively compare the impact of electrolyte on the thermodynamic and electrokinetic properties of host-guest inclusion complexation based on measured  $K_B$  and  $\mu_{ep, AC}$  parameters. The interaction of TESMR was examined by ACE using three model guest corticosteroids, namely hydrocortisone (HC: 1), cortisone (C: 2) and corticosterone (CC: 3) as depicted in Fig. 3.4. Because of the improved sensitivity and resolution of CE using UV detection relative to NMR, simultaneous analysis of all three corticosteroids using micromolar concentrations levels in aqueous solution was realized in a single run. Fig. 3.5 demonstrates differential binding of corticosteroids using TESMR as both an intrinsic buffer and electrokinetic host by ACE. Neutral corticosteroids co-migrate with the EOF when using 0 mM TESMR (*i.e.*, phosphate, pH 7.5) in Fig. 3.5(a), however the use of increasing concentrations of TESMR at pH 7.5



**Fig. 3.5** (a) Differential interaction of corticosteroids using TESMR as intrinsic buffer and electrokinetic host at pH 7.5 by ACE: (i) 0, (ii) 1, (iii) 2 and (iv) 4 mM TESMR. (b) Non-linear regression of the binding isotherms using average viscosity-corrected mobilities ( $n = 3$ ) of corticosteroids based on 1:1 dynamic complexation with TESMR as described in eq. 1. Guest numbering corresponds to: 1-HC, 2-C and 3-CC.

(without phosphate) results in significant mobility shifts and longer migration times due to an increasing fraction of the complex being formed as described in eq. (1). It is apparent in **Fig. 3.5(a)** that baseline resolution of the corticosteroid mixture is achieved using 1 mM TESMR under 4 min by ACE. Moreover, a comparison of the binding isotherms shown in **Fig. 3.5(b)** clearly shows that selectivity is based on  $K_B$  and  $\mu_{ep, AC}$  reflected by differences in the curvature and saturation mobility of the binding isotherms, respectively as summarized in **Table 3.1**. TESMR displays moderate yet differential affinity for the corticosteroid derivatives despite minor differences in chemical structure and bulky size of guests. ACE is unique for enhancing molecular recognition processes relative to conventional techniques since both thermodynamic ( $K_B$ ) and electrokinetic ( $\mu_{ep, AC}$ ) factors can additively contribute to greater selectivity. It is important to note that correction factors due to relative changes in the dielectric strength of the buffer medium caused by host/receptor addition is relevant only for weakly interacting charged/ionic analytes whose mobility are normalized throughout the entire binding isotherm [10]. However, in this study, neutral corticosteroid substrates with zero free mobility were examined with no observed deviations in the measured binding isotherms. The accuracy of apparent binding constant measurements by ACE using TESMR as an intrinsic buffer was also confirmed independently by  $^1\text{H-NMR}$  experiments, which resulted in an average  $K$  of  $(208 \pm 8)$  for HC using its H4; H18 and H19 proton resonance peaks, as shown in **Fig. 3.6**. The three resolved HC proton resonance peaks that were not overlapped by TESMR or solvent signals corresponded to H4 ( $\text{CH}$ , 5.693 ppm), H18 ( $\text{CH}_3$ , 1.316 ppm) and H19 ( $\text{CH}_3$ , 0.760 ppm). All proton resonances were observed to undergo lower

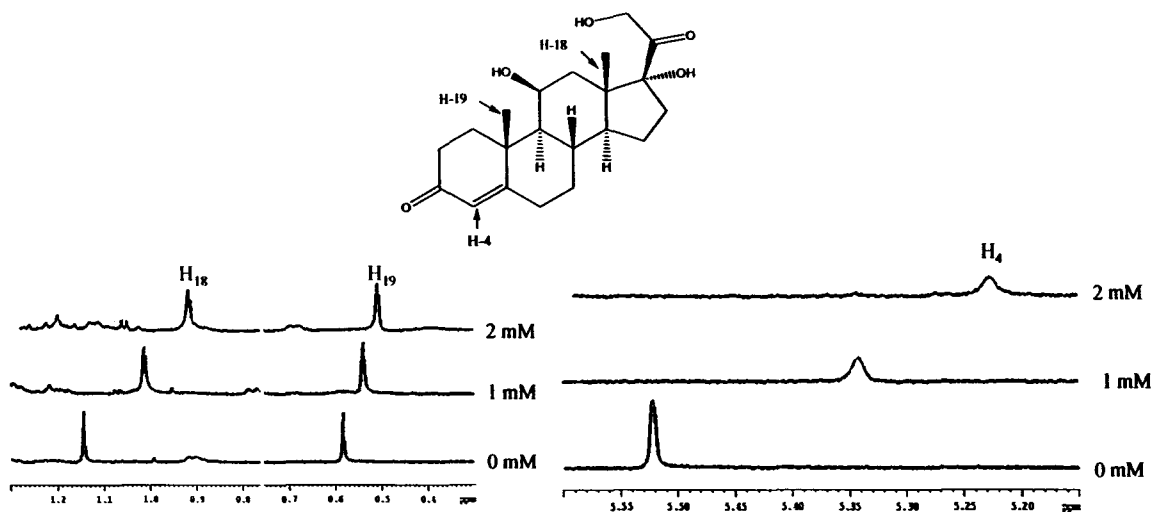
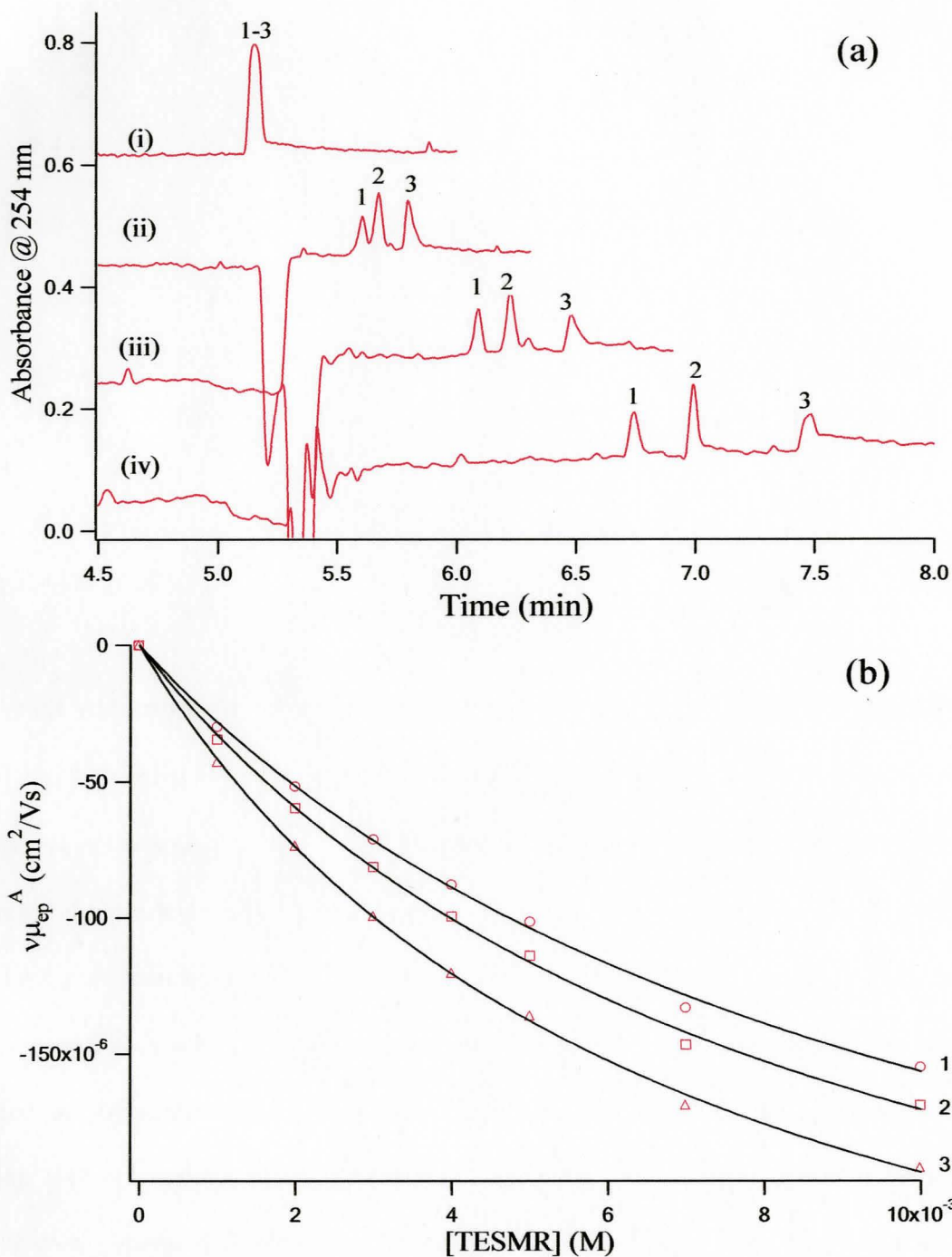


Fig. 3.6  $^1\text{H}$ -NMR complexation-induced chemical shifts of hydrocortisone in the presence of increasing concentrations of TESMR

frequency complexation-induced chemical shifts with TESMR.

### 3.5.3 Reduced apparent binding affinity in extrinsic buffer system

The same experiment as Fig. 3.5 was also performed using 20 mM sodium phosphate, pH 7.5 as an extrinsic buffer in all solutions by ACE. As depicted in Fig. 3.7, the binding isotherms demonstrated that corticosteroids have significantly weaker affinity (about 200 %) for TESMR in an extrinsic electrolyte system at the same pH, as reflected by a more shallow slope in the non-linear binding curves. Note that all electropherograms in Fig. 3.7 were observed to have a slower EOF due to the increased ionic strength of phosphate buffer relative the intrinsic TESMR system in Fig 3.5(a). Although electrolytes are generally required for pH buffer control, as well as altering receptor solubilization and conformational properties (*e.g.*, protein folding), they can also have a detrimental impact on the apparent binding affinity involving host-guest non-covalent interactions. The use



**Fig. 3.7** (a) Differential interaction of corticosteroids using TESMR as an electrokinetic host in 20 mM sodium phosphate buffer, pH 7.5 by ACE: (i) 0, (ii) 1, (iii) 2 and (iv) 4 mM TESMR. (b) Non-linear regression of the binding isotherms using average viscosity-corrected mobilities ( $n = 3$ ) of corticosteroids based on 1:1 dynamic inclusion complexation with TESMR as described in eq. 1.

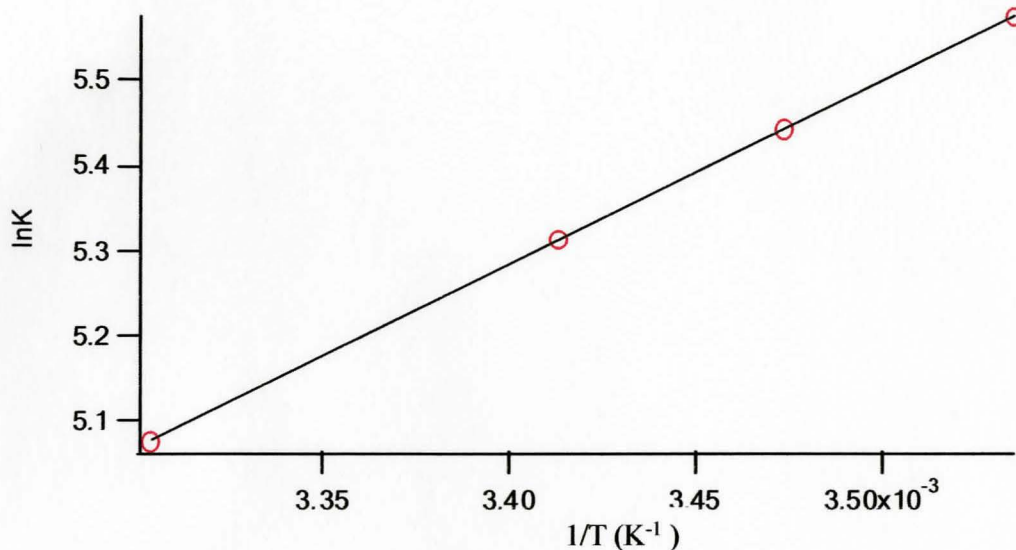


**Fig. 3.8** Van't Hoff plot for the determination of enthalpy and entropy parameters involved in TESMR-HC interaction using the HC methyl-18 chemical shifts by <sup>1</sup>H-NMR.

of high concentrations of electrolytes (*e.g.*, Na<sup>+</sup>) can reduce TESMR-corticosteroid affinity by decreasing the extent of ion-dipole, dipole-dipole and CH- $\pi$  non-covalent interactions in aqueous solution by electrostatic shielding or changes in solvation (*i.e.*, electric double layer) of the anionic host, TESMR [30]. For example, the TESMR-HC affinity was reduced to  $(97 \pm 8)$  in the sodium phosphate buffer system as compared to  $(212 \pm 14)$  when using TESMR as an intrinsic buffer. A Van't Hoff plot was constructed based on the temperature-dependence on the measured TESMR:HC binding constant using H18 resonance peak of HC as depicted in **Fig. 3.8**. Linear regression of the van Hoff plot generated a slope,  $m = (2164 \pm 5)$ , y-intercept,  $b = (-2.07 \pm 0.02)$  and correlation coefficient ( $R^2$ ) = 0.9999. Indeed, thermodynamic data performed by <sup>1</sup>H-NMR reveal that TESMR-HC interaction is enthalpy driven [27] reflected by  $\Delta H^\circ$  (-4.30

$\pm 0.01$ ) and  $T\Delta S^\circ$  ( $-1.22 \pm 0.01$ ) kcalmol<sup>-1</sup> at room temperature, unlike the commonly ascribed hydrophobic effect [29], which is entropically favored by release of bound water upon complexation. Hence, enhanced molecular recognition of enthalpy-driven processes in aqueous solution is realized when using TESMR as an intrinsic buffer without high concentrations of extrinsic electrolytes, which results in stronger binding and complexes of unique mobility for improved selectivity. Further studies will be carried out to more thoroughly examine the impact of ionic strength and ion type used in buffers composed of extrinsic electrolytes on the apparent binding constant derived by ACE measurements.

### 3.5.4 Conformational size selectivity in ACE

Table 3.1 highlights the comparison of the apparent binding and complex mobility parameters measured in this study. It is evident that reduced apparent binding of neutral corticosteroids to TESMR occurs in the presence of 20 mM sodium phosphate buffer. However there was no significant change in the selectivity based on affinity alone since the binding constants of guests were equally affected. Nevertheless, the measured mobility of corticosteroid-TESMR inclusion complexes ( $\mu_{ep, AC}$ ) provide a greater overall selectivity in the case of TESMR as an intrinsic buffer, whereas  $\mu_{ep, AC}$  values were similar in magnitude when using sodium phosphate buffer. Hence, improved selectivity and separation resolution was achieved when using TESMR as an intrinsic buffer without extrinsic electrolytes based on the distinct conformational properties of the complex. In fact, up to 30 % of the overall selectivity in ACE was influenced by the unique

**Table 3.1** Enhanced molecular recognition of corticosteroids based on thermodynamic & conformational selectivity with TESMR as intrinsic buffer and electrokinetic host.

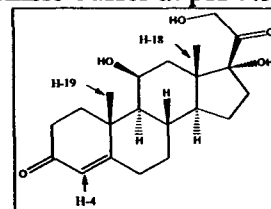
Condition/Analyte	$K_B$ ( $M^{-1}$ )	$\mu_{epAC} \times 10^{-4}$ ( $cm^2V^{-1}s^{-1}$ )	$1 - \mu_{ep, AC} / \mu_{ep, C}$ (%)
<i>(a) TESMR, pH 7.5</i>			
HC	(212 ± 14)	(-3.02 ± 0.10)	(21.4 ± 0.7)
C	(252 ± 16)	(-3.15 ± 0.10)	(18.0 ± 0.6)
CC	(300 ± 18)	(-3.40 ± 0.09)	(11.5 ± 0.3)
<i>(b) Phosphate, pH 7.5</i>			
HC	(97 ± 8)	(-3.17 ± 0.17)	(17.4 ± 0.9)
C	(115 ± 8)	(-3.18 ± 0.14)	(17.2 ± 0.8)
CC	(148 ± 7)	(-3.24 ± 0.08)	(15.6 ± 0.4)

All parameters were calculated using non-linear regression analysis of viscosity-corrected apparent steroid mobilities based on triplicate measurements, where the error represents the standard deviation.

The free mobility of TESMR at pH 7.5 was measured to be  $-3.840 \times 10^{-4} cm^2V^{-1}s^{-1}$

**Table 3.2**  $^1H$ -NMR binding data for HC using TESMR as an intrinsic buffer at pH 7.5

$^1H$ Environment of HC*	Chemical $K_{AC}$ ( $M^{-1}$ )	$\Delta_{max}$ (ppm)
H4	(214 ± 2)	(-0.813 ± 0.005)
H18	(202 ± 4)	(-0.638 ± 0.006)
H19	(209 ± 6)	(-0.209 ± 0.003)



\* Only three major HC proton resonances were resolved from TESMR and solvent peaks in 600 MHz  $^1H$ -NMR spectra

electrokinetic properties of the complex as demonstrated in Table 3.1 (a). In the case of a charged host-neutral guest system, the reduction of the free mobility of TESMR ( $\mu_{ep, C}$ ) is inversely related to a net increase in the hydrodynamic radius ( $R_H$ ) of the complex upon binding with bulky corticosteroids. Table 3.1 also highlights the relative change in complexation-induced mobility or  $(1 - \mu_{ep, AC} / \mu_{ep, C})$ , which is a measure of the size selectivity in ACE based on a spherically-shaped complex. Despite the similar structural properties among the corticosteroid guests which differ by a single functional group, significant differences in the relative increase in  $R_H$  is apparent ranging from  $(21.4 \pm 0.7)$

% to  $(11.5 \pm 0.3)$  % for TESMR-C and TESMR-CC, respectively. These observations reflect the unique conformational properties of each TESMR-corticosteroid complex and the depth of inclusion complexation that is dependent on steric and non-covalent interactions. Indeed, ACE data demonstrate that stronger binding is directly correlated with complexes of higher negative mobility (smaller  $R_H$ ), which implies more tightly-bound compact inclusion complexes. For instance, there was about a 30 % increase in binding affinity, as well as 10 % decrease in  $R_H$  of TESMR-CC relative to TESMR-HC complex, despite a structural difference of a single hydroxyl moiety. Further studies are required to address the importance of conformational selectivity in ACE experiments involving specific biomolecular interactions with bulky substrates, such as protein-protein interactions.

In order to derive better understanding of the conformational properties of the complex, computer molecular modeling and  $^1\text{H-NMR}$  studies were performed in conjunction with ACE data. Fig. 3.9 depicts a stable conformation of the TESMR-HC complex using computer molecular modeling based on an iterative MM2 force field energy minimization with molecular dynamics. Despite the bulky size of the corticosteroid, a stable complex can be formed along the concave upper rim ( $\sim 10\text{\AA}$ ) of TESMR, with preferential orientation of the enone (H4) moiety of the guest towards the cavity relative to methyl (H18 and H19) residues, respectively. There was a relative increase in molecular radius of about 22.3 % upon complexation when comparing the molecular area of free TESMR with the TESMR-HC complex, which is supported by ACE data in Table 1(a). These observations are also consistent with  $^1\text{H-NMR}$  binding

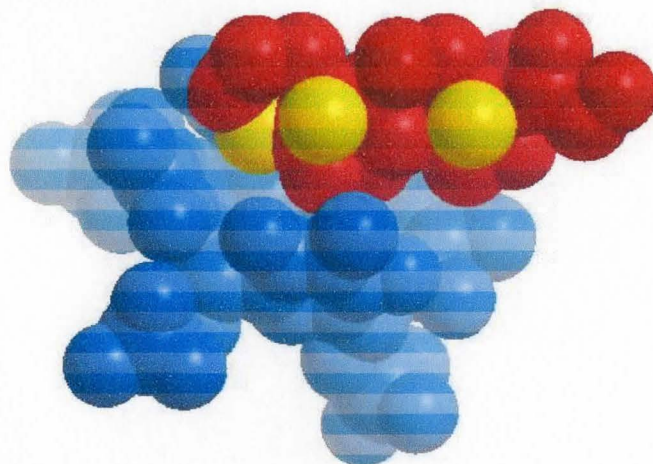


**Fig. 3.9** Energy minimized stable conformation of TESMR (blue):HC (red) inclusion complex with H4, H18 and H19 residues in yellow (left→right).

studies, which generated a  $\Delta_{\max}$  of  $(-0.813 \pm 0.005)$ ,  $(-0.638 \pm 0.006)$  and  $(-0.209 \pm 0.003)$  for H4, H18 and H19, respectively, as listed in **Table 3.2**.  $\Delta_{\max}$  values provide a measure of the relative orientation of inclusion complexation [27], which indicate that the ring-induced anisotropic shielding effects of the TESMR cavity is strongest for C4 and weakest for C19, as indicated in **Fig. 3.9**. It is important to note the distinction between  $\mu_{ep, AC}$  and  $\Delta_{\max}$  parameters derived from CE and NMR experiments, respectively. NMR binding isotherms provide information regarding the orientation of specific proton chemical environments of HC relative to TESMR, whereas ACE data generate average information regarding the hydrodynamic properties of the complex as a whole. Overall, these data suggest that steric and specific  $\pi$ - $\pi$  interactions between the electron-rich aromatic cavity and the conjugated enone of corticosteroids play a vital role in the driving force ( $\Delta H^\circ < 0$ ) for complexation. However, selectivity of TESMR binding is based on weaker dipole interactions with other moieties of the guest, which are dependent on the

electrolyte composition of the solution. Together, ACE, NMR and computer molecular modeling can provide complementary information regarding the conformational properties of complex formation.

### 3.6 Conclusion

Apparent binding constants derived by ACE experiments are relative parameters that are dependent upon the specific buffer composition, including electrolyte type and ionic strength. In this study, about a 200 % enhancement in apparent affinity for a group of neutral corticosteroids was realized when using TESMR as an electrokinetic host and intrinsic buffer at pH 7.5 without additional electrolytes required for pH control and stable ion transport during electrophoresis. Improved selectivity was realized when using TESMR as an intrinsic buffer based on the unique conformational properties of the complex as reflected by the magnitude of  $\mu_{ep, AC}$ . Differences in  $\mu_{ep, AC}$  among similar corticosteroids were attributed to size selectivity in ACE, where there was an inverse correlation between higher affinity and more compact inclusion complexes. The relative change in complexation-induced mobility,  $1 - \mu_{ep, AC}/\mu_{ep, C}$  was used as a parameter to indicate the relative increase in  $R_H$  upon complexation.  $^1H$ -NMR and computer molecular modeling provided additional information regarding the thermodynamics and orientation of the complex. Further studies are needed to better understand the influence of electrolytes in ACE, which can be used for more accurate computer simulations. It is anticipated that receptors that can act as intrinsic buffers will play a more significant role for enhancing molecular recognition in ACE involving a cationic guest-anionic host system, where electrostatic interactions are a dominant factor in complex formation.

### 3.7 References

- [1] Rundlett, K. C.; Armstrong, D. W., *Electrophoresis* **1997**, *18*, 2194-2202.
- [2] Colton, I. J.; Carbeck, J. D.; Rao, J.; Whitesides, G. M., *Electrophoresis* **1998**, *19*, 367-382.
- [3] Heegaard, N. H. H.; Kennedy, R. T., *Electrophoresis* **1999**, *20*, 3122-3133.
- [4] Tanaka, Y.; Terabe, S., *J. Chromatogr. B* **2002**, *768*, 81-92.
- [5] Berezovski, M.; Krylov, S. N., *JACS* **2002**, *124*, 13674-13675.
- [6] Ostergaard, J.; Heegaard, N. H. H., *Electrophoresis* **2003**, *24*, 2903-2913.
- [7] Erim, F. B.; Kraak, J. C., *J. Chromatogr. B* **1998**, *710*, 205-210.
- [8] Villareal, V.; Kaddes, J.; Azad, M.; Zurita, C.; Silva, I.; Hernandez, L.; Rudolph, M.; Gomez, F. A., *Anal. Bioanal. Chem.* **2003**, *376*, 822-831.
- [9] Heegaard, N. H. H.; Nissen, M. H.; Chen, D. D. Y., *Electrophoresis* **2002**, *23*, 815-822.
- [10] Britz-McKibbin, P.; Chen, D. D. Y., *Electrophoresis* **2002**, *23*, 880-888.
- [11] Fang, N.; Chen, D. D. Y., *Anal. Chem.* **2005**, *77*, 840-847.
- [12] Zhu, W.; Vigh, G., *Electrophoresis* **2000**, *21*, 2016-2024.
- [13] Lorenzi, E. D.; Grossi, S.; Massolini, G.; Giorgetti, S.; Mangione, P.; Andreola, A.; Cheti, F.; Bellotti, V.; Caccialanza, G., *Electrophoresis* **2002**, *23*, 918-925.
- [14] Timmerman, P.; Verboom, W.; Reinhoudt, D. N., *Tetrahedron* **1996**, *52*, 2663-2704.
- [15] Román, E.; Peinador, C.; Mendoza, S.; Kaifer, A. E., *J. Org. Chem.* **1999**, *64*, 2577-2578.

- [16] Palmer, L. C.; Shivanyuk, A.; Yamanaka, M.; J.Rebek, J., *Chem. Commun.* **2005**, 7, 857-858.
- [17] Sokoliess.T; Gronau, M.; Menves, U.; Roth, U.; Jira, T., *Electrophoresis* **2003**, 24, 1648-1657.
- [18] Bazzanella, A.; Bachmann, K.; Milbradt, R.; Bohmer, V.; Vogt, W., *Electrophoresis* **1999**, 20, 92-99.
- [19] Britz-McKibbin, P.; Chen, D. D. Y., *Anal. Chem.* **1998**, 70, 907-912.
- [20] Bachmann, K.; Bazzanelle, A.; Haag, I.; Kwang-Yong, H., *Anal. Chem.* **1995**, 67, 1722-1728.
- [21] Kobayashi, K.; Asakawa, Y.; Kato, Y.; Aoyama, Y., *J. Am. Chem. Soc.* **1992**, 114, 10307-10313.
- [22] Siegel, S. C., *J. Allergy Clin. Immunol.* **1985**, 76, 312.
- [23] Nordenstrom, A.; Marcus, C.; Axelson, M.; Wedell, A.; Ritzen, E. M., *J. Clin. Endocrin. Metabolism* **1999**, 84, 1210-1213.
- [24] Terabe, S.; Otsuka, K.; Ando, T., *Anal. Chem.*, **1985**, 57, 834-841.
- [25] Bazzanella, A.; Bachmann, K.; Milbradt, R.; Bohmer, V.; Vogt, W., *Electrophoresis* **1999**, 20, 92-99.
- [26] Bowser, M. T.; Chen, D. D. Y., *Anal. Chem.* **1998**, 70, 3261-3270.
- [27] Gui, X.; Sherran, J. C., *Chem. Comm.* **2001**, 24, 2680-2681.
- [28] Kikuchi, Y.; Kobayashi, K.; Aoyama, Y., *J. Amer. Chem. Soc.* **1992**, 114, 1315-1358.

[29] Higler, I.; Timmerman, P.; Verboom, W.; Reinhoudt, D. N., *J. Org. Chem.* **1996**, *61*, 5920-5931.

[30] Schneider, H. J.; Kramer, R.; Simova, S.; Schneider, U., *J. Amer. Chem. Soc.* **1988**, *110*, 6442-6448.

## CHAPTER 4

### Future Outlook

#### 4.1 Research plans

There are three major areas for future research that warrant further investigation as an extension to this thesis involving the study of thermodynamic and conformational parameters influencing molecular recognition in ACE when using TESMR as a model water-soluble macrocycle. First, a more thorough examination of the influence of electrolyte composition, such as ion strength and buffer co-ion type is required to better understand the impact of extrinsic buffers on  $K_B$  and  $\mu_{ep, AC}$  measurements by ACE. Secondly, a study involving TESMR with a group of cationic guests will be examined in order to demonstrate enhanced affinity when using TESMR as an intrinsic buffer due to the importance of electrostatic interactions. Thirdly, an alternative detection mechanism for non-fluorescent steroids will be developed using TESMR as a probe based on dynamic competitive displacement of a solvophobic dye using CE with indirect LIF detection. In essence, our future plan is to develop a multi-functional macrocycle that serve as an intrinsic buffer, electrokinetic host and probe for sensitive and selective detection of neutral analytes without chemical derivatization by CE-LIF.

#### 4.2 Influence of electrolyte composition

The binding isotherms demonstrated that neutral corticosteroids have significantly weaker affinity (> 200 %) for TESMR in 20 mM sodium phosphate buffer, pH 7.5 due to electrostatic screening effects of additional electrolytes (*i.e.*,  $\text{Na}^+$ ) in solution. However, it

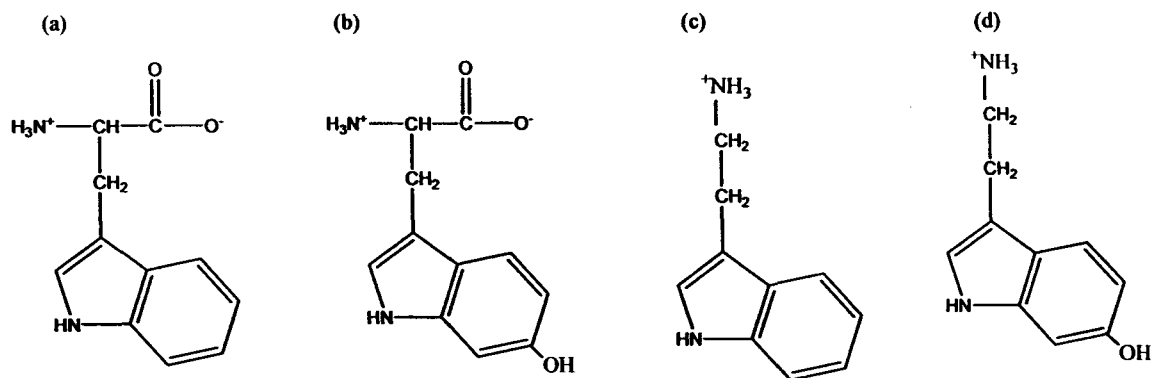


Fig. 4.1 Chemical structures of test guest analytes: (a) tryptophan, (b) hydroxytryptophan, (c) tryptamine, (d) hydroxytryptamine .

is still unclear what property of the solution is most important for modifying apparent affinity. Thus, future investigations will study the impact of electrolytes on the apparent binding of TESMR to guests which will include a more in-depth examination of the impact of ionic strength and cation type (*i.e.*, K<sup>+</sup>, Mg<sup>+2</sup>, NH<sub>4</sub><sup>+</sup>) of the extrinsic buffer at pH 7.5 to better understand the role of electrostatic shielding .

### 4.3 Anionic host:cationic guest model system

A study of the interaction of TESMR to natively fluorescent guests will be examined with specific interest at exploring a charged host-cation guest model system. One of the limitations of using TESMR in CE separations is the strong background UV absorbance of the host, which interferes with the detection of low concentrations of guests. The interaction of TESMR with a group of indoleamines will be investigated by ACE with LINF detection since improved detection and enhanced affinity is anticipated due to their strong native fluorescence and cationic properties, respectively. The chemical structures of the indoleamines are highlighted in Fig. 4.1. Relative to neutral corticosteroids, a

much stronger measured TESMR:indoleamine affinity ( $> 10^3 \text{ M}^{-1}$ ) is expected due to significant electrostatic and  $\pi$ - $\pi$  non-covalent interactions. Moreover, the application of TESMR as an intrinsic buffer and electrokinetic host in ACE will provide significant enhancement in apparent binding since electrostatic interactions are highly dependent on electrolyte composition of the solution. Moreover, it is feasible that the ionic strength composition of an extrinsic buffer can also significantly modify  $\mu_{\text{ep, AC}}$  by changes in the preferred conformation of the inclusion complex via suppression of indoleamine electrostatic interaction with the sulphonated anionic pendant feet of TESMR. In effect, it is foreseen that the ionic strength of the solution may control the complex conformation (*e.g.*,  $R_{\text{H}}$ ) as revealed by ACE between an electrostatic-favored conformer relative to  $\pi$ - $\pi$ -favored conformer.

#### **4.4 TESMR as a probe for indirect fluorescence detection**

TESMR will be used as a probe for indirect detection of non-fluorescent steroids with weak intrinsic chromophores, such as dehydroisoandrosterone (DHEA) by ACE with indirect LIF detection. Thus, TESMR is envisioned to be used as an intrinsic buffer (increase affinity), electrokinetic host (separation of mixtures of neutral steroids) and probe for indirect steroid detection without off-line chemical derivatization. The strategy involves the use of a solvophobic dye (*e.g.*, dansyl amide) that has native fluorescent properties which are extremely sensitive to the surrounding dielectric strength of the medium. A low concentration of dye will be added to an intrinsically buffered TESMR solution and undergo dynamic inclusion complexation with TESMR yielding a steady

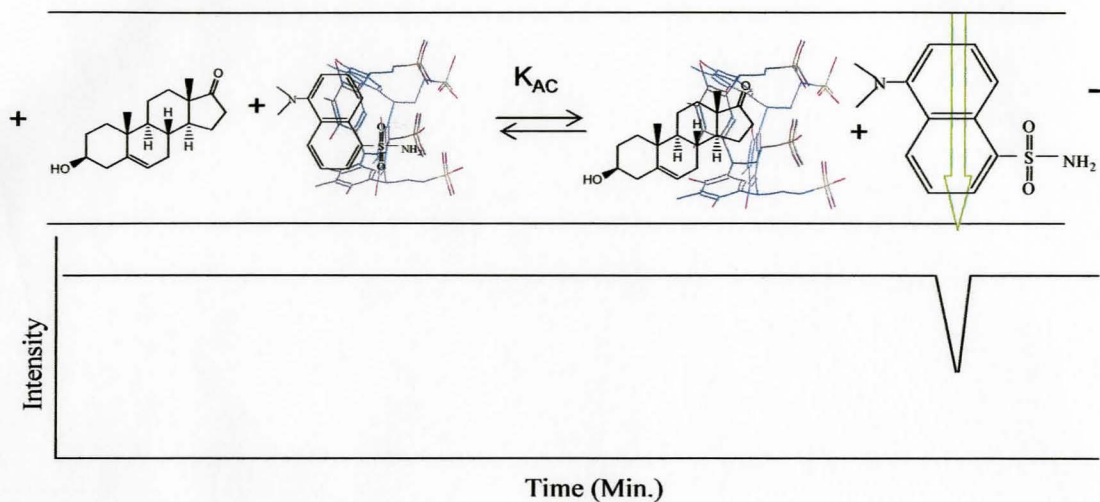


**Fig. 4.2** Pictorial illustration of ACE with indirect LIF detection of DHEA by dynamic complexation with TESMR and displacement of the solvophobic dye dansylamide.

fluorescence background signal due to an equilibrium mixture of free and bound dye. In general, the  $\Phi_F$  of dansyl amide is suppressed in aqueous solution (free state) relative to apolar environment (TESMR bound). Thus, indirect fluorescence detection of DHEA is based on displacement of dansyl amide upon TESMR inclusion complexation during electromigration resulting in a lower fluorescence intensity (negative signal) at the detector window, as illustrated in **Fig. 4.2**. The overall detection limit and sensitivity of the technique will be dependent upon several factors, such as the relative affinity of steroid guest compared to dansyl amide for TESMR which determines the net fraction of dye displaced, as well as the magnitude of  $\Phi_F$  change as a function of solvent polarity. The application of solvophobic dyes that have similar affinity to TESMR as steroid guests ( $\approx 3 \times 10^2 \text{ M}^{-1}$ ) along with large  $\Phi_F$  changes upon inclusion complexation with TESMR will permit single-step and sensitive detection of complex steroid mixtures by ACE-LIF without time-consuming sample pretreatment based on chemical derivatization.